J Stat Phys (2010) 138: 1010–1044
DOI 10.1007/s10955-009-9911-1

Extremal Properties for Weakly Correlated Random Variables Arising in Speckle Patterns

A. Porzio · S. Hüller

Received: 8 September 2009 / Accepted: 16 December 2009 / Published online: 5 January 2010

Abstract Extremal properties of the statistics of speckle pattern are studied in the context of so-called "optically smoothed" light beams of laser-matter interaction. It is shown that the asymptotic statistics of the highest intensity in a speckle pattern, which can be associated with the most intense speckles, follows a Gumbel law, which is in agreement with numerical simulations. It is found that the probability density function of the most intense speckle peaks around the value corresponding to the logarithm of the number of speckles in the considered volume times the average intensity value of the speckle pattern. This result is of great interest for nonlinear processes, like instabilities, where extreme speckles play an important role.

Keywords Order statistics · Extreme theory · Gumbel law · Statistical optics · Speckles

1 Introduction

We study the extremal properties of so-called speckle patterns, namely small-scale structures in a field intensity pattern that are characterized by a statistical distribution of the speckle peak field intensities. We aim to describe the asymptotic behaviour of the maximum of the intensity, that is, the statistical properties of the most intense speckles. These extremal properties, in particular the fluctuation of intensity maxima are an important issue for physics. Many nonlinear mechanisms that involve speckle statistics can be sensitive to the speckle distribution in the upper tail. The latter is for example of great importance in astrophysical observations and in particular for laser matter interaction where instabilities in the beam propagation, like filamentation, or scattering instabilities (see e.g. [1–4]) depend on intense speckles. Due to their threshold-like onset, as a function of intensity, the development of

A. Porzio (✉)
LAGA, Institut Galilée, Université Paris 13, CNRS, 93430 Villetaneuse, France
e-mail: porzio@cpht.polytechnique.fr

A. Porzio · S. Hüller
Centre de Physique Théorique CPHT, CNRS, Ecole Polytechnique, 91128 Palaiseau Cedex, France

such instabilities can yield diverging results, depending on the value of the most intense speckle.

1.1 Physics Background

We focus in the following to the application of extremal properties of speckles for the case of laser-matter interaction. In this context so-called laser "smoothing" techniques are applied to overcome undesired large-scale inhomogeneities that may appear in the profile of the light intensity of generic laser beams that exit from the amplification chain. The term "laser beam smoothing" is commonly used when randomness is introduced in the phase front of high-power laser beams. The result of such smoothing techniques is an overall "smoothness" in the cross section of the beam on a large scale, say over many ($\gg 1$) light wavelengths, while, however, on a shorter spatial scale, say over a few laser wavelengths, the beam is characterized by speckles. Due to the applied smoothing techniques, these speckles are coherent structures of homogeneous size with, of course, statistically distributed intensities. The most frequently used method for spatial smoothing is the so-called 'Random Phase Plate' ("RPP") technique, which produces on the focal plane an intensity pattern consisting of a large number of small-size "speckles", also called 'hot spots', [5–8], see Figs. 1 and 2.

A typical speckle distribution function (DF) can be characterized by the "body", namely the interval where the probability density for speckles peaks, and by the "tail" of the most intense speckles. The body of the distribution, located around the mean speckle intensity, [9–11] is generally a well-known function, which can in the case of laser-smoothing easily be deduced from the experimental technique applied [5–10, 12]. The "body" of the speckle DF depends only very weakly on the quality of the light beam incident to the RPP, i.e. whether the beam is close to an ideal beam (e.g. a plane wave) or whether imperfections in the optical path and/or during the amplification deform the intensity profile and the wave phase front. The "tail" of the distribution, however, contains only a small number of intense speckles (for a finite-size speckle pattern), and hence, statistically, depends delicately on the beam quality and on the information in the RPP mask. The tail may therefore exhibit considerable fluctuations with respect to changes in the phase mask and/or in the optical path.

The optical smoothing methods have been very popular and successful also in theoretical modeling of laser-matter interaction [2, 3, 11, 13]: this is a consequence of the low sensitivity of the body of the DF on details of the laser beams, which were often only poorly

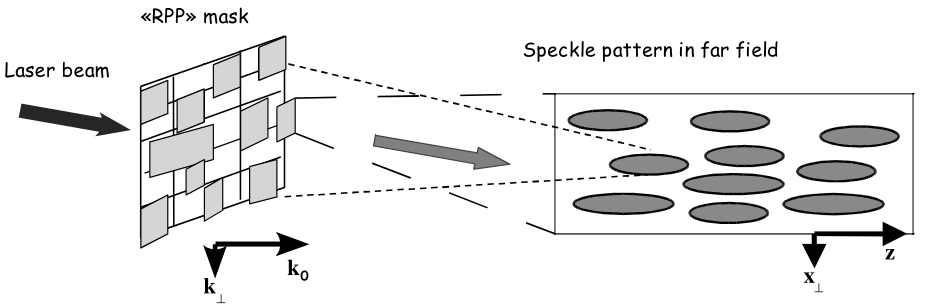

Fig. 1 Illustrative scheme showing the Random Phase Plate mask in the "near field", generating a speckle pattern in the "far field". The overall size of the mask (or of the focusing lense behind) determines the speckle size, while the size of an individual phase element determines the size of the enveloping beam

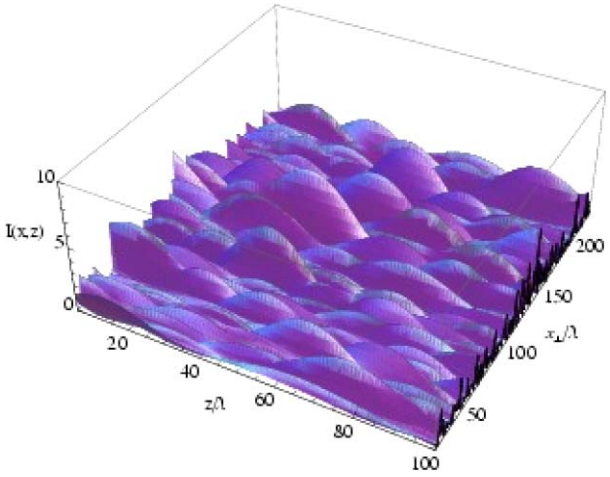

Fig. 2 Illustration of a speckle pattern over the light propagation direction z and one transverse direction $x_\perp$ (both in units of the light wavelength $\lambda_L = 2\pi/k_0$) generated by a Random Phase Plate, with 64 random phase elements, $\kappa = k_0/8$, $r_c = 2\lambda_L$, $\ell_c = 25\lambda_L$. The image shows only a part of the pattern used for the simulations

characterized in laser-matter interaction experiments. From this point of view, the intensity profiles of RPP-smoothed 'generic' laser beams resemble (in the focal plane) surprisingly well to speckle patterns originating from an 'ideal' beam [13–15]. This is the reason why good agreement between theory and experimental results has been found using RPP-smoothed beams where the physics was governed by contributions from speckles in the body of the DF.

For processes, however, with critical dependence on high intensities [1, 4], potentially situated in the tail of the speckle DF, theoretical modeling is often difficult because of the incomplete information from experiments. A statistical treatment of the fluctuations in the tail of the speckle DF is therefore necessary, and the study of extremal properties in the tail of the DF is very valuable for such critical processes.

1.2 Extremal Properties

For this purpose we study the extremal properties of Gaussian random fields (and related random fields) which have been investigated earlier in [16] and [17, 18], and have been, more recently, in [11, 19, 20], applied to laser-matter (plasma) interaction.

The approach chosen for our work is motivated by the fact that the maximum of a speckle field is expected to follow an extreme value distribution [21], in our case a *Gumbel* (or double-exponential) law. Knowing this feature, one has to determine the particular form of the Gumbel law for the case of weakly correlated structures like speckles, as done in Sects. 2.3 and 2.4. Our approach is hence different from [11, 19, 20]. There are two further aspects from which our approach is distinct from previous work, namely: (1) we study the extremal properties of the intensity in speckle patterns by considering correlations via phases (instead of considering real and imaginary parts of the fields), and (2) we use a discretised spatial mesh to resolve the speckle pattern by going into the limit of high resolution, such that the correlation inside speckles is an issue. The latter is different from Adler's approach [17] used in [11, 19, 20].

In the work presented here, we will hence elaborate how the most intense speckle in a speckle pattern, which we call from now *principal intensity maximum*, follows a so-called *Gumbel* (or double-exponential) law.

It is known [21–27] that the Gumbel law describes the statistics of the maximum value M_n of a sequence $\{I_n\} = I_1, \ldots, I_n$ of exponentially distributed intensity values,

$M_n \equiv \max(I_1, \ldots, I_n)$. In the here considered case, this sequence corresponds to n points taken from a mesh spanned over the speckle pattern.

Let us remark here a further aspect that distinguishes our approach from previous work: we intend to determine the maximum of the speckle pattern, however, we need not require that the values of the sequence $\{I_n\}$ are itself maxima.

Generally, the value M_n is not identical with the *principal intensity maximum*, associated with the most intense speckle, as long as the number of points n is small compared to the number of points of a highly resolved mesh characterizing the speckle pattern. We will show, however, that in the limit of high resolution, the statistics of the *principal intensity maximum* follows a Gumbel law, although the condition for *non-clustering* (see later), due to the coherent structure inside a spatially resolved individual speckle, is not fulfilled. This result is underlined by numerical simulations demonstrating an excellent agreement with the Gumbel law. Numerical simulations are based on a great number of realisations of an algorithm generating a (highly resolved) speckle pattern corresponding to the one of a beam generated by a Random Phase Plate.

The article is organized as follows: In Sect. 2, we first recall the notion of paraxial light wave propagation in presence of beam smoothing techniques, which we develop for the example of random phase elements in the phase front. The resulting correlation properties of light fields are of importance to the application of the notions of extreme statistics that are developed in the following section, together with a discussion on the convergence toward a Gumbel law. In Sect. 3 we compare the theoretical results on the asymptotic behaviour of the most intense speckle with numerical simulations. In Sect. 4 we evaluate the joint probability densities of the random intensities $(I_1, \ldots, I_n)$ by successively developing the covariance matrix for point-to-point correlations on a regular, ordered mesh. This successive derivation will be generalized in Sect. 7, after having proven that the joint distribution of the $I_1, \ldots, I_n$ has the required properties to establish the convergence of the distribution of the maximum term of the sequence, $M_n = \max(I_1, \ldots, I_n)$. This is done in Sect. 5 by examining the decay of the covariance matrix, reflecting the correlation of speckle light fields. Furthermore, in Sect. 6, we discuss the behaviour of the "total intensity" of the light field with respect to the maxima. We conclude in Sect. 8.

2 Model Definitions: Light Propagation and Extreme Statistics

2.1 Paraxial Propagation and Correlations

We recall in this section the properties of paraxial wave propagation which allows to evaluate the correlation in the speckle field pattern for a light beam, generated with random phase elements, in the vicinity of the focus of the overall light beam.

Light fields are solutions to the hyperbolic wave equation for the field E:

$$(\partial_\zeta^2 + \partial_x^2 - c^{-2}\partial_t^2)E = 0 \tag{1}$$

which in complex representation, has the form $E(x, \zeta, t) = a(x, \zeta, t)e^{i\psi}$ for a solution propagating in one direction. (For the moment and for simplicity we restrict ourselves to two spatial dimensions, one parallel to the propagation axis ζ, the other, x, transverse to the ζ-axis.) For a quasi-monochromatic source, the phase ψ can be written as $\psi = ik_0\zeta - i\omega t$ where the wave vector k_0 denotes the component in the propagation direction and ω is the corresponding frequency.

For not strongly focused beams with the single principal propagation direction ζ, and the transverse dimension x, (1) can be simplified by the so-called paraxial approximation for the complex field $a(x, \zeta, t)$, which reads for a forward-going solution of the field E

$$\left[2ik_0\left(\partial_\zeta + \frac{\omega}{c^2 k_0}\partial_t\right) + \partial_x^2 + \left(\frac{\omega^2}{c^2} - k_0^2\right)\right]a = 0, \tag{2}$$

where k_0 and ω are chosen such that $\omega^2/c^2 - k_0^2 \equiv 0$, as in a homogeneous medium or the vacuum.

The corresponding solution of a light field composed by speckles can be written as the superposition of an ensemble of complex fields a_m, all with the same propagator $e^{ik_0\zeta - i\omega t}$, but with distinct values in the transverse direction. The phase is shifted in x and z direction upon the individual initial phase φ_m, $E(x, \zeta, t) = \sum_m a_m \exp\{i\psi + ik_m x - ik_m^2\zeta/2 + i\varphi_m\}$, where k_m is now the wave vector component in the transverse direction, and $k_m^2/2k_0 \simeq k_0 - [k_0^2 - k_m^2]^{1/2}$ is the correction to the wave vector along the propagation axis (remind that $k_m^2 \ll k_0^2$ for validity of this paraxial approximation). For convenience, we restrict ourselves to the stationary solution, such that the term $\partial_\zeta + (\omega/c^2 k_0)\partial_t$ reduces to a simple derivative in ζ (which is however equivalent to the solution in the frame $\zeta - c_g t$ with the group velocity $c_g \equiv c^2 k_0/\omega$).

Furthermore, here and in the following, the x axis has been normalized to k_0^{-1}, the ζ axis to $k_0/\sqrt{2}$, such that $k_0 x \to x$ and $k_0\zeta/\sqrt{2} \to z$. The field describes, in paraxial approximation, the propagation from the so-called "near field", where the speckle-generating "Random Phase Plate" is situated, $\sum_m a_m e^{i\varphi_m}$, towards the "far field" $A(x, z)$ in the focal plane, see Fig. 1.

In the far field representation, the correlation function, $\mathcal{E}(A(x, z)A(x', z'))$, between fields in two points with coordinates (x, z) and (x', z') is the essential quantity to evaluate the covariance matrix C which allows to determine the *joint probability density*

$$p(\underline{A}) = \frac{1}{(2\pi)^n\sqrt{|C|}}\exp\left(-\frac{1}{2}(\underline{A} - \bar{\underline{A}})^t C^{-1}(\underline{A} - \bar{\underline{A}})\right) \tag{3}$$

with the vector $\underline{A} = \{A_1, A_2, \ldots, A_n\}$ spanned by the components corresponding to the fields in the points $(x_1, z_1) \ldots (x_n, z_n)$, and with $\bar{\underline{A}}$ being the expectation value for the random fields (which can be assumed to be zero in the current contexts $\bar{\underline{A}} = 0$ [9, 10, 16]). C is a $2n \times 2n$ matrix (see [11, 19, 20]) with the 2×2 block elements:

$$\begin{aligned}
C^{rr}(x, z, x', z') &= \mathcal{E}(\mathrm{Re}\, A(x, z)\, \mathrm{Re}\, A(x', z'))\Delta_c,\\
C^{ii}(x, z, x', z') &= \mathcal{E}(\mathrm{Im}\, A(x, z)\, \mathrm{Im}\, A(x', z'))\Delta_c,\\
C^{ri}(x, z, x', z') &= \mathcal{E}(\mathrm{Re}\, A(x, z)\, \mathrm{Im}\, A(x', z'))\Delta_c, \quad \text{and}\\
C^{ir}(x, z, x', z') &= \mathcal{E}(\mathrm{Im}\, A(x, z)\, \mathrm{Re}\, A(x', z'))\Delta_c,
\end{aligned}$$

with $\Delta_c = 1/\mathcal{E}(|A(x, z)|^2)$.

Later on, we will discuss the details of the joint probability density depending on the correlation between the field values measured in different points. For this reason the complex field quantity $A(x, z)$ needs to be evaluated from the solution of the light propagation. After propagation toward the "far field" in the focal volume, the superposition of the fields from the phase plate elements yields $A(x, z) = \sum_k a_k \exp\{ikx - ik^2 z + i\phi_k\}$, [11] where we can assume that the phases ϕ_k are uniformly distributed on $[-\pi, \pi]$.

For the example of real-real correlations we obtain:

$$\begin{aligned}&\mathcal{E}(\mathrm{Re}\,A(x,z)\,\mathrm{Re}\,A(x',z'))\\&=\int_{-\pi}^{\pi}\sum_k\sum_h |a_k||a_h|\cos(kx-k^2z+\phi_k)\cos(hx'-h^2z'+\phi_h)d\phi\\&=\sum_k |a_k|^2\big[\cos(k(x-x'))\cos(k^2(z-z'))+\sin(k(x-x'))\sin(k^2(z-z'))\big],\end{aligned}\quad(4)$$

and hence $\Delta_c = 1/(2\sum_k |a_k|^2)$.

Before we discuss the joint probability density for higher order correlations, let us just recall that the *marginal probability density* for such fields is simply given by an exponential law,

$$p(I)\propto \exp -\lambda I,\quad(5)$$

where $I = (\mathrm{Re}\,A(x,z))^2 + (\mathrm{Im}\,A(x,z))^2$ is the intensity of the light field in any point of the field pattern.

In the following we shall principally refer to the case of the so-called 'flat-top' amplitude model in the 'near field' with $a_k = const \equiv 1$ within the interval $|k| = [0,\kappa]$ for the transverse wave number, and $a_k = 0$ elsewhere. In polar coordinates this yields (see §4, formula (18)) for the correlation:

$$\mathcal{E}(\mathrm{Re}\,A(x,z)\,\mathrm{Re}\,A(x',z')) = \int_0^{\kappa}\rho\cos(\rho^2 z)\mathcal{J}_0(\rho x)d\rho.\quad(6)$$

With the help of the latter expression one can compute the typical speckle size, which is a measure of the spatial extension inside which field values are correlated. The importance of the knowledge of the correlation function is two-fold: (i) on a "long" range the convergence of the covariance matrix is necessary in order that the joint probability density, see (3), exists; (ii) the "clustering" of points at which the intensity is evaluated inside a coherent structure like a speckle, has an impact on the shape of the limit law.

The proof of the (i) 'long' range convergence is subject of Sects. 4–5, whereas the (ii) 'clustering' inside the speckles, being an important notion for the shape of the distribution function, is discussed in the following section.

By determining the typical speckle size via the correlation function, one can compute the specific speckle volume with respect to the overall volume considered. In simulations, for instance, the specific speckle volume depends on the spatial dimensions involved (2D or 3D), as does the simulation volume. Therefore the ratio *Volume/specific Volume* determines the number of speckles, n_{sp} potentially to be observed. The latter will be shown to be an important parameter in the following. Its value will be concretized in Sect. 3.2 on the simulation results.

In this context it is important to note, that due to the paraxial approximation the cutoff value of κ in the wave number transverse to the propagation direction must be small (compared to the total wave vector) in order to maintain the validity of this approximation, namely to derive (2) from (1). In general, this cutoff is related to the so-called optical 'f-number', $f\#$, such that $\kappa \equiv 1/2f\#$. The paraxial approximation is valid for $f\# > 2$, hence the condition for the cutoff reads $\kappa < 1/4$.

Let us furthermore remark that the autocorrelation, $\mathcal{E}(AA^*)$ for the present case is a so-called 'flat top' amplitude in the 'near field' $a_k = const$ within $k = [0,\kappa]$, and it is just the

result of the solution for the case of coherent field components ($\phi_k \equiv 0$), namely

$$A_c(x,z) = \int_0^\kappa \exp(-ik^2 z) k \, \mathcal{J}_0(kx) dk,$$

i.e. $|A_c(x,z)| \equiv |C^{rr}(x,0,z,0) + iC^{ri}(x,0,z,0)|$ or $\mathrm{Re}\, A_c(x,z) \equiv \mathcal{E}(A(x,z)A(x,z)^*)$.

In the general case, where $a_k(k)$ is the amplitude distribution of the uncorrelated and $a_{k,c}$ of the coherent 'near field', the autocorrelation and the coherent field solution A_c are related as [11],

$$\begin{aligned} \mathrm{Re}\, A_c(x,z) &= \int_0^\infty a_{k,c}(k) \cos(k^2 z) k \, \mathcal{J}_0(kx) dk \\ &\equiv \int_0^\infty |a_k(k)|^2 \cos(k^2 z) k \, \mathcal{J}_0(kx) dk = \mathcal{E}(A(x,z)A(x,z)^*), \end{aligned} \tag{7}$$

for $|a_k(k)| \equiv \sqrt{|a_{k,c}(k)|}$ using $\mathcal{E}(A(x,z)A(x,z)^*) = 2\mathcal{E}(\mathrm{Re}\, A(x,z)\, \mathrm{Re}\, A(x,z))$. In pratice, for the concrete and illustrative case of a Gaussian light "beam", $A_{k,c} \propto e^{-k^2 w_c^2}$, $|a_k| \propto e^{-k^2 w^2}$ the width in the uncorrelated case, w, relates to the width in the coherent case as $w = w_c/\sqrt{2}$. The value of w has its equivalence to the 'flat-top' case with (in dimensionless units) the $w = 2\pi f\# = \pi/\kappa$.

2.2 The Extreme Statistics and the Gumbel Law

We consider a speckle pattern of a laser light beam generated by a so-called Random Phase Plate. The field intensity profile of this pattern can be considered as a set of a great number of random values following a statistical distribution, the marginal probability density of which is an exponential (5). For the extreme statistics of the speckle pattern we hence consider a sequence of random measurements $\{I_n\} \equiv I_1, \ldots, I_n$, characterising the intensity in n points of the speckle pattern.

We denote with $H_n(x)$ the probability distribution $P(M_n < x)$ for the maxima $M_n = \max(I_1, \ldots, I_n)$ of a sequence of n points H_n, expressing namely the probability that the value M_n is found below the value x. We wish to evaluate the *asymptotic* distribution $H(x)$ of the maxima M_n for $n \to \infty$. To obtain a non-degenerate limit law of the distribution (not reducing to values 0 or 1), one has to find a suitable transform $M_n \to (M_n - a_n)/b_n$ for the maximum values M_n with the rescaling coefficient b_n and the shift a_n. The transform allows to relate the distribution for the maximum M_n (finite n) to a limit law for $n \to \infty$ as $\lim_{n\to\infty} H_n(a_n + b_n x) = H(x)$ with an adequate function $H(x)$, provided that a choice for a_n and b_n exists. The latter express the probability limit $\lim_{n\to\infty} P((M_n - a_n)/b_n < x)$, which is, introducing $u_n = a_n + b_n x$, equivalent to $\lim_{n\to\infty} P(M_n < u_n)$.

For the distribution function $F(u_n)$ (with the complementary distribution $\bar{F}(u_n) \equiv 1 - F(u_n)$), describing the probability $P(I_j < u_n)$ that a value I_j of the sequence $\{I_n\}$ is below u_n, the average number of exceedences of the level u_n is given by $P(\{I_n\} > u_n) = n\bar{F}(u_n)$. If and only if a choice for a_n and b_n is possible such that the value of $n\bar{F}(u_n)$ stabilizes with n toward a positive real value τ, one can find a limit as

$$\lim_{n\to\infty} n\bar{F}(u_n) = \tau \quad \text{with } \tau \in (0, \infty). \tag{8}$$

If the n values of $\{I_n\}$ are independent, the probability that the maximum of all, M_n, stays below u_n, is consequently given by

$$P(M_n < u_n) = \prod_{j=1}^{n} \big(1 - \bar{F}(u_n)\big) = \big(1 - \bar{F}(u_n)\big)^n \tag{9}$$

which yields, using (8), that $P(M_n < u_n) = (1 - (\tau/n) + o(1/n))^n \to \exp(-\tau)$ with $o(1/n)$ being a residual value decreasing faster than $1/n$. The latter expresses the existence of a limit law H for the maximum M_n, and it is equivalent to the existence of the average number of exceedences in the sequence [21].

Now, for the exponential distribution being the representative distribution of the intensity values in the speckle pattern, i.e. $F(x) = 1 - e^{-\lambda x}$ (λ standing here for the average intensity) and $\bar{F}(x) = e^{-\lambda x}$, we have $\bar{F}(a_n + b_n x) = \exp(-\lambda a_n)\exp(-\lambda b_n x)$. Obviously, a good choice for the coefficients is $a_n = (1/\lambda)\log n$ and $b_n = 1/\lambda$ yielding

$$n\bar{F}(u_n) = \exp(-x) \quad \text{with } u_n = \frac{x + \log n}{\lambda}, \tag{10}$$

because $P(M_n < u_n)$ reads now

$$P(M_n < u_n) = \left(1 - \frac{e^{-x}}{n}\right)^n \to \exp(-e^{-x}) \quad \text{with } n \to \infty. \tag{11}$$

The limit law $\lim_{n\to\infty} P(M_n < u_n)$, corresponding to the maxima of the sequence $\{I_n\}$ of intensities in the speckle pattern, is hence the *Gumbel* (or double exponential) law $H(x) \equiv \exp(-e^{-x})$ [21, 22].

In particular the coefficient a_n, involving the log of the number of points n, will be important in the following, in order to relate the Gumbel law to the distribution H for finite n.

In an asymptotic limit in n of the sequence $\{I_n\}$ and for a highly resolved mesh, as discussed later, our derivation still holds. For this asymptotic case, the absence of independence in the sequence $I_1, \ldots, I_n$ is, however, an issue, but we can still have a limit theorem for the distribution of the maximum: this is precised by two conditions, a first one, *condition 1*, on the decay of long range correlations, and a second, *condition 2*, on the short range which allows not too many joint exceedences of a given level [21, 24, 27, 28]. It has to be remarked that, when both conditions are satisfied we have the same limit behaviour for M_n, with the same $u_n = (\log n + x)/\lambda$ as in the independent case. When merely *condition 1* is satisfied, the situation is more involved, what is the subject of the following sections.

2.3 Case of a Sequence $I_1, \ldots, I_n$ in Absence of Independence

Indeed, when $I_1, \ldots, I_n$ are not independent, but have the same common distribution function F, we can still state a limit theorem, provided that the sequence of I_i's is not so far from an independent sequence. This is what is expressed by *conditions 1* and *2*:

Condition 1 or "the joint distribution of $\{I_i\}$ about mixing in the upper tail", states that the joint distribution function defined as $F_{i_1\ldots i_n}(u_n) \equiv P(I_1 < u_n, \ldots, I_n < u_n)$ the distribution function of $I_1, \ldots, I_n$ for that all values $I_1, \ldots, I_n$ are below the value u_n satisfies the following inequality:

$$|F_{i_1,\ldots,i_k,j_1,\ldots,j_t}(u) \; - \; F_{i_1,\ldots,i_k}(u) \cdot F_{j_1,\ldots,j_t}(u)| \le \tau(s,u) \tag{12}$$

where for the sub-sequences $I_{i_1}, \ldots, I_{i_k}$ and $I_{j_1}, \ldots, I_{j_t}$ with $1 < i_1 < \cdots < i_k, i_k + s < j_1 < \cdots < j_t$ (i.e. separated by s), the value of $\tau(s, u)$ is such that for $u_n \to \infty$ there exists a sequence $s_n \to \infty$ such that $\tau(s_n, u_n) \to 0$ when $n \to \infty$ [21, 24, 27].

We prove this condition in Appendix A. *Condition 1* is a distributional mixing condition, weaker than most classical forms of dependence. It applies on the 'long range', restricting (long range) dependence, as it weakens range-m dependence (i.e. I_i and I_j independent for $|i - j| > m$) in that the dependence is small but non-zero. It weakens mixing, as prescribes the decay of correlations only on suitable sequences of values of the intensities going to infinity. Hence, it is a condition of mixing adapted to the extreme value problems for which only the upper tail of the distribution is relevant.

Condition 2 is the "non-clustering condition" and applies on the 'short range', restricting the clustering of high level exceedences. It bounds the probability of more than one exceedence on a block of given length (N), so that joint exceedences (in clusters) become more and more unlikely.

Precisely, for $n \equiv NM$, let u_{NM} be the NM-th element of the sequence u_n, split in M packages of length N, of *condition 1*, $N \in \mathbb{N}^*$, $M \in \mathbb{N}^*$; then *condition 2* reads:

$$\limsup_{N \to \infty} N \sum_{j=2}^{N} P(I_1 > u_{NM}, I_j > u_{NM}) = o\left(\frac{1}{M}\right) \tag{13}$$

as $M \to \infty$. This non-clustering property will be proven and discussed in Appendix B.

Indeed, for $n = NM$ we obtain from (8) $NP(I_i > u_{NM}) \to \exp(-x)/M$. This means that by splitting a sequence of NM indexed intensity values in M packets of length N, for a packet of N indexed intensity values there are, in average, $O(1/M)$ exceedences of the level u_{NM} by a single I_i. Looking now for exceedences in pairs we find in case of an independent sequence, that the number of pair exceedences is bounded by $N \sum_{j=2}^{N} P(I_1 > u_{NM}, I_j > u_{NM}) \to \exp(-2x)/M^2$. In the lack of independence, we still wish to have a bound on pair exceedences, in order to prove that the asymptotic behaviour of the maximum M_n is the same as in the independent case. This is the meaning of expression (13) for $M \to \infty$, which "allows" more joint exceedences than in the independent case, but less than single exceedences. This condition gives a threshold criterion when one passes from $o(1/M)$ to $O(1/M)$, when expressed in terms of the development of the correlation coefficient around the unity value, see Appendix B.

The "non-clustering" *condition 2* is an important issue when taking limit of sequences $I_1, \ldots, I_n$ in a speckle pattern toward *high resolution*, where the ensemble of all n points resolves even individual speckles, which are itself correlated. For this purpose, let us define the number of 'potential' speckles in a volume by n_{sp}. For a concrete definition let us refer to Sects. 3 and 3.2 where we discuss the numerical simulations. *High resolution* in these terms means that $n \gg n_{\mathrm{sp}}$, and, in practice, allows to converge toward the distribution of the *principal intensity maximum*. Let us distinguish the cases

(i) for *low* resolution $n < n_{\mathrm{sp}}$, and
(ii) for *high* resolution $n > 2n_{\mathrm{sp}}$,

for which the splitting of n measured intensity values in $M > 1$ packages of length N can be used.

2.4 Recentering of the Gumbel Distribution: Meaning of the Shift

Indeed, the approach consisting in choosing n points in a volume and then looking for the statistics of the maximum value among these n points is a starting point to investigate the

statistics of the global maximum in the box. For the sequence $I_1, \ldots, I_n$ of intensities it is known that, under *conditions 1* and *2*, the limit distribution is a Gumbel law with shift in intensity controlled by the number of points n.

Under the case defined above (i) $n < n_{\mathrm{sp}}$, the shift in intensity of the Gumbel law is strictly defined by (10), i.e. $\propto \log n$ for $n \ll n_{\mathrm{sp}}$.

In case (ii) the non-clustering *condition 2* is no longer fulfilled. At this point, as the speckle has a coherent structure, it is clear that the shift in a Gumbel distribution (which corresponds to the position in intensity of the maximum of the probability density) can no longer be proportional to the total number of points, for instance, the number of grid points resolved. Intuitively, it is clear that the result must be stable with respect to the resolution, once the resolution is fine enough to resolve the structure of a speckle.

It is known from [27, 28] that under *condition 1* only, any limit distribution of the max of the sequence $I_1, \ldots, I_N$ has to be a Gumbel law

$$H^{\theta}(x) = \exp\{-\theta \exp(-x)\} \quad \text{with } 0 < \theta < 1. \tag{14}$$

This means that *condition 2*, interpreted as a function of the development in the correlation coefficient, can explain the change in the parameter θ from $\theta = 1$ to $\theta < 1$. This change has a unique effect, the change of the shift from $\log n$ [case (i)] to $\log(n/\theta)$ [case (ii)]. Indeed, $H^{\theta}(x) = H(cx + d)$ with $c = 1$ and $d = \log \frac{1}{\theta}$ and $P(M_n < a_n + b_n x) \to H(x)$ with $a_n = \log n/\lambda$ and $b_n = 1/\lambda$ if

$$P(M_n < c_n + d_n x) = \left(1 - e^{-\lambda(c_n + d_n x)}\right)^n \to_{n\to\infty} H^{\theta}(x) \tag{15}$$

with $c_n = \log(n/\theta)/\lambda$ and $d_n = 1/\lambda$.

The criterion when θ has to be chosen different from unity, because *condition 2* is not satisfied, can be inferred by an analysis as performed in Appendix B. This criterion is obtained by performing a development as a function of the correlation coefficient between two points, and it shows nicely the tendency that θ decreases toward small positive values as the pair correlations increase with the total number of points (in the same volume).

Condition 2 is indeed not satisfied inside a speckle structure, however, from the above discussion, it is clear that still a Gumbel law following expression (14) can be used for the extremal statistics we aim to describe. The value of θ acts as a shift in intensity $\propto \log\theta$ which centers the Gumbel distribution different from the case (i).

For an illustration of the shift showing the change of the parameter θ we refer to Table 1 and to the section where we present the simulation results. If $n < n_{\mathrm{sp}}$, then $\theta = 1$, i.e. the number of points on which measures are taken is lower than n_{sp}, so that the shift is $\log n$ in the Gumbel distribution. As n approaches, $n \simeq n_{\mathrm{sp}}$ and exceeds n_{sp}, the shift stabilizes

Table 1 Summary of θ values in H^{θ}, as well as of $(1 + \frac{n}{n_{\mathrm{sp}}})\theta$, as a function of the dimension n of the sequence $I_1, \ldots, I_n$. The values are taken on n equally distributed points in a speckle pattern resolved by 80384 grid points, and are based on 500 realisations of the speckle pattern. n varies between $n = 100$ and $n = 80000$, close to the resolution of the grid. The number n_{sp} of potential individual speckles in the volume is $n_{\mathrm{sp}} \simeq 2500$. The values of θ are deduced from numerical simulations by adjusting θ to yield the least-square fit to the probability density $dH^{\theta}(u)/du$

n	100	200	400	800	1600	3200	6400	12800	25600	51200	80000
θ	0.99	0.99	0.85	0.68	0.57	0.43	0.28	0.17	0.10	0.05	0.03
$(1 + \frac{n}{n_{\mathrm{sp}}})\theta$	1.03	1.08	0.98	0.89	0.94	0.99	1.00	1.07	1.09	1.12	1.12

to attain an asymptotic value for $n > n_{sp}$. In anticipation of our numerical results, we find that $\theta = 1$ in case (i) for $n < n_{sp}$, while in case (ii) the behaviour of θ as a function of n follows $\theta n_{sp}/n$ for large n/n_{sp} ratios. As seen from Table 1, a good compromise to cover both regimes, even with non-integer values of n/n_{sp}, is $\theta(1 + n/n_{sp}) \simeq 1 \simeq const.$

Physically this stabilisation means that the maximum of the measured intensity values on n points inside a speckle pattern cannot exceed the global maximum intensity value of the considered speckle pattern.

3 Convergence Toward the Law of Gumbel: Comparison with Simulations

It is the subject of this section to relate the extremal properties discussed above to the simulation results for a large number of realisations of speckle patterns, from which the statistics of the *principal maximum*, having the highest local maximum, can be derived considering the tail of the speckle distribution function. Let us remind that more than any other local maximum in the speckle pattern, the intensity of the most intense speckle may show important fluctuations from one to another realisation of speckle patterns. Exchanging phase plates in a RPP array particularly affects the principal intensity maximum, while the statistical properties at lower field intensities remain almost unchanged. We furthermore recall the properties of the joint distribution function to show that the probability distribution for the principal maximum converges toward a Gumbel law. The conditions for the convergence will be made explicit in Sect. 4 where the joint distribution function will be worked out for a set of random intensities in our model.

3.1 Gumbel Law for the Principal Maximum

The theorem given by (15) yields for a sequence of intensity values $I_1, \ldots, I_n$ with $n \gg 1$ (i.e. measured on a high density of points in a speckle pattern, such that individual speckles are resolved), the probability

$$P(\max(I_1, \ldots, I_n) < u) \simeq H^{\theta}(u - \log n) = \exp(-n\theta e^{-u}) = \exp(-\theta e^{-(u-\log n)}). \quad (16)$$

As already mentioned earlier, see Sect. 2.2, the sequence $I_1, \ldots, I_n$ for a given number n is not intended to contain the global maximum of a speckle pattern. We will, however, show in the following, that it is possible to derive the distribution of the *principal maximum of a speckle pattern* from this theorem, namely by refining the density of points inside the speckle pattern. Expressions (15) and (16) allow to find a Gumbel distribution corresponding to the maximum of the sequence $I_1, \ldots, I_n$, namely $M_n = \max(I_1, \ldots, I_n)$, even if points around this maximum are registered within the sequence. This allows to go toward the limit that individual speckles are highly resolved, so that M_n is very close to the absolute maximum of the speckle pattern considered. Refining the density of points again, say from $n \to Kn$ on the same pattern, $K > 1$, will no more change the value such that $|M_n - M_{Kn}|/M_n = o(1/K)$. In this limit, we can state that the distribution of M_n, being a Gumbel distribution and centered around $u = (\log n - \log \theta)$ in (16), converges toward the distribution of the *principal intensity maximum* of the speckle pattern.

We have carefully verified the properties of the Gumbel distribution for a sequence $I_1, \ldots, I_n$ in speckle patterns numerically. By going toward the limit of very high resolution we can confirm the properties announced above.

3.2 Simulation Results

In our simulations aiming to determine the distribution function of the *principal intensity maximum*, the Random Phase Plate is characterized by

(1) the focusing aperture, determining the cutoff in the wave vector $|k_m| < \kappa$, and
(2) the number $n\#$ of phase plate elements, thus causing a subdivision of the wave vector k_m in intervals with $n\#$ random phase values. See for illustration Figs. 1, 2.

The cutoff in k_m determines, like for an individual speckle (i.e. equivalent to a single phase plate), the size of the speckle, namely $r_c = \beta_\perp w = \beta_\perp \pi/\kappa$ in width (being $\beta_\perp f\#\lambda_L$ in dimensional units) and $\ell_c = \beta_\parallel k_0 r_c^2/2$ in length (in dimensional units) [19, 20], with $\beta_\perp$ and $\beta_\parallel$, being constants of the order of unity, depending on the shape of the RPP, as defined by the a_k-values in (4) in Sect. 2.1. The number $n\#$ determines the potential overall size of the beam, namely $W = \pi/n\#k_0 \gg r_c$ for its width for numerous phase plate elements. We use the method of a usual RPP, where the phases jump randomly between 0 and π (but in practice also random values can be used with the same properties). The potential number of speckles in a given volume $n_{\rm sp}$ is therefore given by $\alpha(L_\perp/r_c)^{d_\perp} L_\parallel/\ell_c$ with $d_\perp$ standing for the dimensions considered in the direction perpendicular to the propagation, and with α being a numerical factor of order unity, $\alpha \simeq 2\pi$ for $d_\perp = 1$.

We first study the statistical properties of the sequence $I_1, \ldots, I_n$ where the values are taken at n arbitrarily chosen points on a mesh in space on which the speckle intensity pattern was computed. The mesh resolution was extremely fine. In a first step, the number of points n is small compared to the total number of mesh points N_m. This ensures that both *conditions 1* and *2* are fulfilled, such that the Gumbel law must hold.

We show evidence for the validity of the Gumbel law by two sets of simulations:

(1) we keep the volume of the simulation box and the number of mesh points N_m constant, and determine the distribution for sequences $I_1, \ldots, I_n$ by increasing the number of points n from $n \ll N_m$ toward $n \leq N_m$;
(2) we consider two simulation boxes, the second box having twice the volume of the first one, in which we take a sequence $I_1, \ldots, I_{2n}$ twice as long compared to the one of the first box. We keep, however, the same resolution such that $N_m^{(2\text{nd})} = 2N_m^{(1\text{st})}$.

The computed probability distributions clearly exhibit a shape of a Gumbel distribution. Furthermore, increasing the number of points of the sequence, leads to a shift of the center of the distribution in intensity, as suggests (16). Both sets of simulations confirm this feature, (1) the first showing a shift by steps of $\log 2$ in intensity when increasing the number of points n each time by a factor of 2, namely $n = 100$, 200, 400, and 800, see Fig. 3. The second set (2) shows similarly a shift of $\log 2$, as expected, see Fig. 4.

Figure 3 shows the distributions for the maximum of the sequence $M_n = \max\{I_1, \ldots, I_n\}$ from 500 realisations of a RPP-generated speckle pattern. By successively increasing n beyond $n = 800$ in set (1), one can observe a convergence of the distribution curves in Fig. 3: although n is successively increased always by a factor of 2, the distance between the curves in intensity is less than $\log 2$ for $n = 800$, 1600 and 3200. For $n = 6400, \ldots, n = 51200$, and $n = 80000$ the curves almost merge toward a unique one, giving evidence for a convergence toward a distribution that is independent of the increment in the number of points (up to the total number of mesh points $N_m = 80384$ for the case shown). This is what we would expect to happen: a convergence toward the distribution representing the *principal intensity maximum* once the mesh is sufficiently fine to resolve individual speckles. Consequently, taking always the maximum value in intensity of all the N_m points resolved of the overall

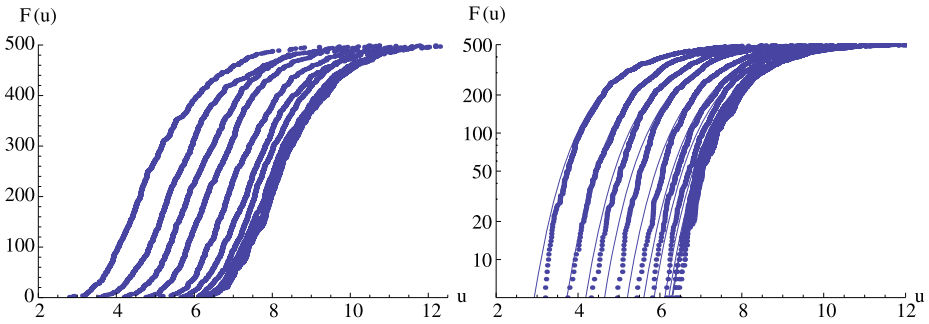

Fig. 3 Probability distributions $F(u)$ (multiplied by the number of realisations) for the maximum of the sequence $I_1, \ldots, I_n$ as a function of the intensity, normalized to the mean intensity of the pattern, from 500 realisations of a RPP-generated speckle pattern. *Left subplot* linear scale, *right subplot* logarithmic scale in the number of counts (note that the value of F, usually normalized to unity for $u \to \infty$ is multiplied by purpose by the number of realisations). The *dotted curves*, from *left* to the *right*, show the distribution for $n = 100$, 200, 400, 800, 1600, 3200, 6400, 12800, 25600, 51200, and 80000 points, respectively. (The total number of mesh points was, however, with $N_m = 80384$ considerably higher.) The *solid lines* correspond to a Gumbel distributions corresponding to the least square fit to each curve. The potential number of speckles in the volume is $n_{\mathrm{sp}} \simeq 2500$

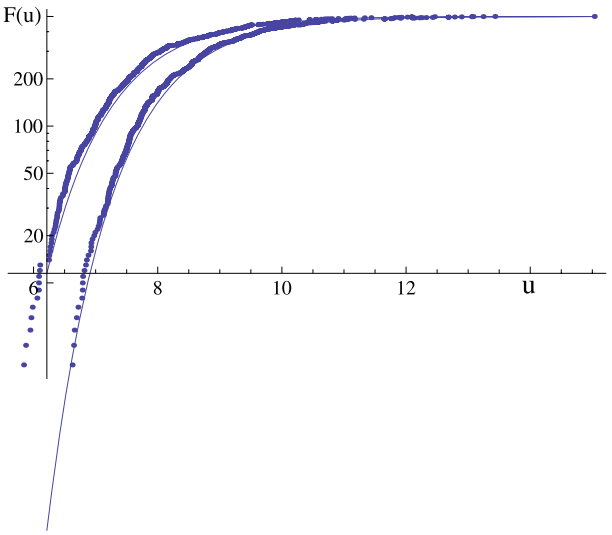

Fig. 4 Probability distributions for the maximum of the sequence $I_1, \ldots, I_n$ as a function of the normalized intensity u from 500 realisations of a RPP-generated speckle pattern on a logarithmic scale in the number of counts (F is again multiplied by the number of realisations). The *curves* are distinguished by the number of points $n = 800$ and 1600, but of twice the volume for the latter. *Both curves* are hence shifted by $\log 2$ in intensity. (The total number of mesh points was, however, with $N_m = 80384$ considerably higher, and $n_{\mathrm{sp}} \simeq 2500$)

speckle pattern, over a large number of realisations, numerically yields the distribution of the *principal intensity maximum*. For the example shown in Fig. 3 it is indistinguishable from the curve for $n = 80000$.

The shape of all computed distributions is for each case very close to a Gumbel distribution. As evoked earlier when we have introduced the Gumbel law with the parameter θ, the distribution for values n small such that the non-clustering criterion is fulfilled, i.e. $\theta \equiv 1$, the shift in intensity must follow $\log n$, while a Gumbel law of the type H^θ holds if the non-clustering criterion is not fulfilled, which is obviously the case for $n > 1600$ in the simulations shown.

Let us comment on the convergence toward a unique distribution for a highly resolved mesh: This convergence beyond a sufficiently good resolution is evident when considering

that the speckle structure close to an intensity maximum is correlated and has a parabolic shape around the maximum as a function of the distance (in $x_\perp$ or z in our notation), namely $\propto I_{\max}(1 - x_\perp^2/r_h^2)$ (and similarly in z) where r_h is numerically close to r_c[1] (and ℓ_c in z) [19, 20]. The error in the intensity value, ΔI, with respect to $I_{\max}$ converges hence rapidly with $(\Delta x)^2$, and thus with $1/K^2$, for a resolution $\Delta x = r_c/K$ with $K > 1$ indicating the number of grid points inside r_c. For $\Delta x > r_c$, however, the error goes in general with Δx. The requirement that the error in the intensity value I is inferior to the value of the mean intensity, $\langle I \rangle$, of the overall field pattern is hence $\Delta x_\perp/r_c < (I/\langle I \rangle)^{-1/2}$, which is $\Delta x_\perp < r_c/3$ for typical values. This criterion ensures that for N_m sufficiently high, the sequence $I_1 \ldots, I_n$ with $n \to N_m$ contains a value M_n very close to the value of the *principal intensity maximum*. Of course, in case of a too coarse resolution the intensity peak value can be missed, falsifying the scale of the distribution function aiming to represent the *principal intensity maximum*.

3.2.1 Interpretation of the Table 1 and Discussion

From the different distributions for the various number of sequences $I_1, \ldots, I_n$ for $n = 100, \ldots, 80000$ we have determined a least square fit to both (i) a Gumbel distribution following $H^\theta(I)$ in (16) and (15) and (ii) the corresponding probability density $dH^\theta(I)/dI$, by seeking for the best value of θ fitting the numerical data. The corresponding values for θ are summarized in Table 1 and in Fig. 5. We furthermore show the good agreement between a Gumbel distribution and its probability density with the numerically computed values, see Fig. 6. Let us comment here on the interpretation of Table 1. As it is explained in Sect. 2.4, the non-clustering *condition 2* is not fulfilled for a sufficiently high density of points in the vicinity of the coherent structure of a speckle. We have shown that still a Gumbel distribution of the form H^θ applies, where θ is decreasing toward smaller positive values with

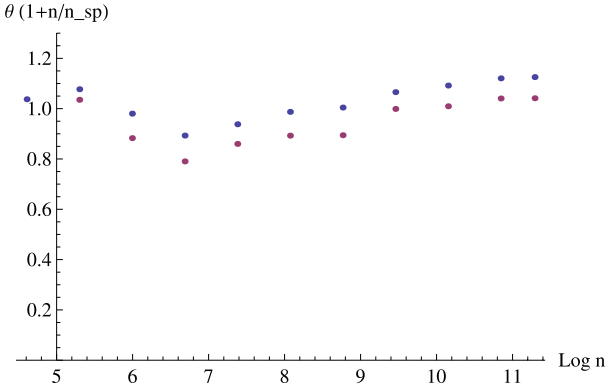

Fig. 5 Value of the parameter θ determined as a function of the number of points n considered for the sequence $I_1, \ldots, I_n$, multiplied by $(1 + n/n_{\rm sp})$ as in Table 1. The data are determined with the help of a least square fit from two sets of numerical data, namely: between the numerical data for the probability distribution, shown in Fig. 3, and the Gumbel distribution $H^\theta(u)$, and between the probability density derived from the distribution values and $dH^\theta(I)/dI$, respectively. Both sets show very close results, yielding values of $(1 + n/n_{\rm sp})\theta$ close to unity, as expected

[1] For a 'flat top' RPP, e.g. the expectation value of the speckle radius is greater than the radius r_h of the parabolic behaviour around the intensity peak. The latter, however, has to be resolved to find M_n.

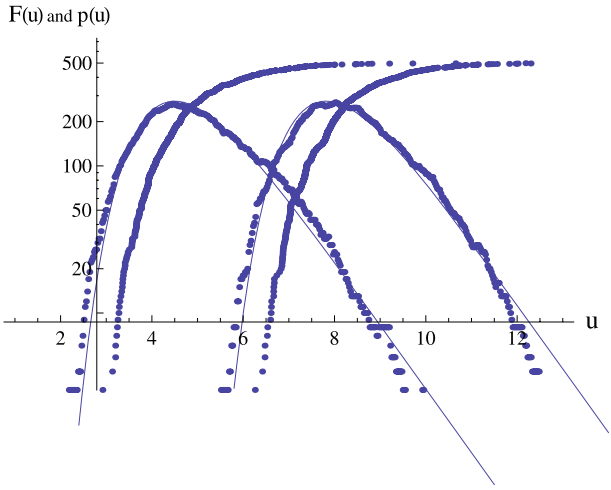

Fig. 6 In Logarithmic scale: Distribution $F(u)$ and its probability density $p = dF/du$ (both multiplied by the number of 500 realisations) as a function of the normalized intensity u for the two extremes $n = 100$ and $n = 80000$, the latter representing the *principal intensity maximum*, computed from 500 realisations of an optically RPP-smoothed light field; the *solid curves* show the corresponding Gumbel probability density following $p_\theta(u)$ of (18), centered around the (normalized) intensity value $u \sim \log n_{\rm sp} \simeq 7.8$. The total number of mesh points is 80384, the number of potential speckles in the volume is $n_{\rm sp} \sim 2500$

increasing correlation. We observe in Table 1, that multiplying θ with the factor $1 + n/n_{\rm sp}$, which is $\simeq n/n_{\rm sp} \gg 1$, results in an almost constant value very close to unity,

$$(1 + n/n_{\rm sp})\theta \simeq const \simeq 1. \tag{17}$$

We can use this hence as a better approximation for θ than what we have obtained by an approximate procedure in Appendix B.

Denoting n as the total number of observed points, we know that for the maximum of the sequence M_n holds

$$P(M_n \le u) \sim \exp(-n\theta e^{-u}) = \exp(-e^{-(u-\log n\theta)}),$$

which yields after a change of parameters $P(M_n \le x/\lambda + \log(n/\theta)/\lambda) \to \exp(-\theta e^{-x}) = H^\theta(x)$. By considering the dependence of θ on the ratio $n/n_{\rm sp}$, either using the first approximation found in Appendix B, or better the expression (17) deduced from our simulations,

$$\exp(-n\theta e^{-u}) = \exp\{-e^{-u}\ n\ n_{\rm sp}/(n + n_{\rm sp})\}.$$

This eventually means that the distribution of the *principal intensity maximum* is given by a Gumbel law following H^θ with (17) resulting in the behaviour $\theta \to n_{\rm sp}/n$ for $n/n_{\rm sp} \gg 1$, so that $P(M_n \le u) \sim \exp\{-n\theta e^{-u}\} \sim \exp\{-e^{-(u-\log n_{\rm sp})}\}$ and thus yielding the probability density

$$p_\theta(u) = \exp[-(u - \log n_{\rm sp}) - e^{-(u-\log n_{\rm sp})}]. \tag{18}$$

Physically the shift which stabilises around a value $\log n_{\rm sp}$ independent of n has a clear meaning. It depends on the number of speckles potentially found in a given volume. The value around which the probability density is centered must be clearly superior to the average intensity of the field and of all speckles. The probability density $p_\theta(I)$ also rapidly decreases in intensity with $\exp[-\delta I \exp(-\delta I)]$, for $\delta I < 0$ (using $\delta I = u - \ln n_{\rm sp}$), i.e. showing an almost threshold-like onset "left" of the peak value of the $p_\theta(u)$. In the other limit, for $\delta I > 0$, for higher intensities, beyond its peak, the density $p_\theta(u)$ decreases close to an exponential tail, but slightly slower.

The very good agreement of our simulations with (16) and (18), both on a linear as on a logarithmic scale (!), makes it evident that for an adequate choice of the parameter θ, the Gumbel law is the natural description for the probability distribution of the principal intensity maximum. Let us underline that the Gumbel law provides an exact expression of an extremal law, and that the only approximation to be used in (16) and (18) comes from the evaluation of the parameter θ. This value enters only as a logarithmic (i.e. weak) dependence on the number of speckles n_{sp} in the shift in intensity of the peak value of $p(u)$, and it refers to a concrete and intuitive physical meaning.

4 The Covariance Matrix and Correlations

In the previous sections, we have introduced the Gumbel law as limit law for the most intense maximum of a speckle pattern. In order to prove the convergence toward a Gumbel law, we proceed in determining the correlations in between points of the speckle pattern, which eventually allows to determine the covariance matrix and the joint probability density.

Based on the paraxial propagation of light waves developed earlier, and on which the demonstration of the Gumbel law was shown in the previous section, we proceed to derive the correlations and henceforth the covariance matrix related to the probability density.

We transform the sum in (4) into an integral and change for $x = (x_1, x_2)$ and $k = (k_1, k_2)$ into polar variables $k_1 = \rho\cos\theta$ $k_2 = \rho\sin\theta$ and $k \cdot x = x_1\rho\cos\theta + x_2\rho\sin\theta = \rho|x|\cos\alpha$ for suitable α. For a 'flat top' distribution of the amplitudes a_k, with $a_k = const \equiv 1$ within a radius $\rho \le \kappa$ (and $a_k = 0$ elsewhere) this results in

$$\begin{aligned}\mathcal{E}(\mathrm{Re}\,A(x,z)\,\mathrm{Re}\,A(x',z')) &= \int_0^\kappa \rho\cos(\rho^2 z)\int_0^{2\pi}\cos(\rho x\cos\alpha)d\alpha d\rho \\ &\quad + \int_0^\kappa \rho\sin(\rho^2 z)\int_0^{2\pi}\sin(\rho x\cos\alpha)d\alpha d\rho \\ &= \int_0^\kappa \rho\cos(\rho^2 z)\mathcal{J}_0(\rho x)d\rho. \end{aligned} \tag{19}$$

Suppose that the speckle field is represented, in the far field, close to the light beam focus, by the amplitudes $\{A_1, A_2, \ldots, A_n\}$ at points $1 \ldots n$ in the (x, z) plane, and consider the values as a sequence of complex random variables, where $A_j = (A_j^i, A_j^r)$ represents the field at the point $P_j \equiv (x_j, z_j)$. The complex field values A_k relate to the intensity I_j at P_j as follows $\sqrt{I_j}\cos(t_j) = A_j^r$ and $\sqrt{I_j}\sin(t_j) = A_j^i$. Starting from the definition for the correlation between the real parts of the field, $E(\mathrm{Re}\,A(x,z)\,\mathrm{Re}\,A(x',z')) = C^{rr}(x,z,x',z')$, we proceed in the same way for the other correlations. Hence, we obtain for the joint density of $\underline{A} = \{A_1, A_2, \ldots, A_n\}$

$$p(\underline{A}) = \frac{1}{(2\pi)^n\sqrt{|C|}}\exp\left(-\frac{1}{2}(\underline{A}-\bar{\underline{A}})^t C^{-1}(\underline{A}-\bar{\underline{A}})\right) \tag{20}$$

where C is the $2n \times 2n$ covariance matrix (see [11, 19, 20]) with the 2×2 block elements:

$$\begin{aligned} C^{rr}(x,z,x',z') &= \int_0^\kappa k\cos(k^2(z-z'))\mathcal{J}_0(k(x-x'))dk = C^{ii}(x,z,x',z'), \\ C^{ri}(x,z,x',z') &= \textstyle\int_0^\kappa k\sin(k^2(z'-z))\mathcal{J}_0(k(x-x'))dk = -C^{ir}(x,z,x',z'). \end{aligned} \tag{21}$$

Note that $A_n = (A_n^r, A_n^i)$ is called a circular complex random variable; in particular the correlations between the points P_n and P_m obey $C^{ri}(P_n, P_m) = -C^{ir}(P_n, P_m)$ and $C^{ri} = -C^{ir} = 0$ for $P_n = P_m$.

For what follows, it is important to evaluate the decay of the correlations with increasing distance between points. Let $\xi = z - z'$ and $\eta = x - x'$ then the correlation coefficient R_{ij} between the points $i = P(x, z)$ and $j = P(x', z')$ decreases as

$$R_{ij} \leq const \cdot \left(\frac{1}{|\xi|} + \frac{1}{|\eta|^{\frac{3}{2}}} \right).$$

Note that the step sizes required to evaluate the correlation between points P_n and P_m are not necessarily small, such that the individual speckle size is resolved. The grid sizes chosen to find the individual maxima of a speckle pattern, as done in Sect. 3 have been chosen much finer than the distance between P_n and P_m. The correlation coefficient of the inverse matrix decreases at the same speed (see below in Sect. 5). Indeed, the coefficients R_{ij} measure the correlation between two points i and j of the plane. A discretised evaluation of the correlation (or covariance) matrix, however, requires an ordering in the distance between the points. Hence, in a two-dimensional plane considered here, we have chosen to follow a representative cut for the ordering in a single dimension, in each direction.

We will proceed in estimating the coefficients, with the x-section and the z-section of the correlation matrix, representing the strength, or the decay of the correlation with respect to the x direction or the z direction. Physically, this represents the directions along and transverse the light wave propagation.

4.1 Correlations in the Simplified Case with $C^{ri} = -C^{ir} = 0$

We start by computing the joint density of the intensities in the—by a technical point of view—simpler case where $C^{ri} = -C^{ir} = 0$, and we refer to a later section to consider the general case, $C^{ri} = -C^{ir} \neq 0$. In the following we discuss in detail the cases with $n = 2$ and $n = 3$.

4.1.1 Example $n = 2$ (see [9])

Recall that $A_j = (A_j^i, A_j^r)$ represents the field at the point P_j. Then, for $n = 2$ we compute the joint density of the variables I_1, I_2

$$C = \begin{pmatrix} \sigma^2 & 0 & \mu & \delta \\ 0 & \sigma^2 & -\delta & \mu \\ \mu & -\delta & \sigma^2 & 0 \\ \delta & \mu & 0 & \sigma^2 \end{pmatrix}, \tag{22}$$

with $\mu \equiv C^{rr} = C^{ii}$ for $P_n \neq P_m$, $\sigma^2 \equiv C^{rr}$ for the autocorrelation ($P_n = P_m$), and $\delta \equiv C^{ri}$. We consider now the simplified case of a real-valued matrix with $\delta = 0$ together with $\sigma^2 = 1$, yielding

$$p(I_1, I_2, t_1, t_2) = \frac{1}{2\sqrt{|C|}4\pi^2} \exp\left\{ \frac{-1}{2(1-\mu^2)} (I_1 + I_2 - 2\mu\sqrt{I_1 I_2}\cos(t_1 - t_2)) \right\} \tag{23}$$

and

$$p(I_1, I_2) = \frac{1}{2} \frac{1}{2(1-\mu^2)} \exp\left\{ \frac{-1}{2(1-\mu^2)} (I_1 + I_2) \right\} \mathcal{I}_0\left(\frac{\mu}{1-\mu^2} \sqrt{I_1 I_2} \right). \tag{24}$$

Let us remark that the marginal density of I_1 is defined as

$$p(I_1) = \frac{1}{2}\exp\left\{-\frac{1}{2}I_1\right\} \tag{25}$$

which is exponential with $\lambda = 1/2$ and $\sigma^2 \equiv 1/2\lambda = 1$.

4.1.2 Example $n = 3$ with $C^{ri} = -C^{ir} = 0$

For the case $n = 3$ the covariance matrix reads

$$C = \begin{pmatrix} 1 & 0 & R_{12} & 0 & R_{13} & 0 \\ 0 & 1 & 0 & R_{12} & 0 & R_{13} \\ R_{12} & 0 & 1 & 0 & R_{23} & 0 \\ 0 & R_{12} & 0 & 1 & 0 & R_{23} \\ R_{13} & 0 & R_{23} & 0 & 1 & 0 \\ 0 & R_{12} & 0 & R_{13} & 0 & 1 \end{pmatrix} \tag{26}$$

so that the joint density is

$$\begin{aligned} &p(I_1, I_2, I_3, t_1, t_2, t_3) \\ &\quad = \frac{|J|}{\Delta(2\pi)^3} e^{\frac{-I_1}{\Delta}(1-R_{23}^2)} e^{\frac{-I_2}{\Delta}(1-R_{13}^2)} e^{\frac{-I_3}{\Delta}(1-R_{12}^2)} \\ &\qquad \cdot e^{\frac{2}{\Delta}(R_{12}-R_{23}R_{13})\sqrt{I_1 I_2}\cos(t_1-t_2)} e^{\frac{2}{\Delta}(R_{13}-R_{12}R_{23})\sqrt{I_1 I_3}\cos(t_1-t_3)} e^{\frac{2}{\Delta}(R_{23}-R_{13}R_{12})\sqrt{I_2 I_3}\cos(t_2-t_3)} \end{aligned} \tag{27}$$

where $\Delta^2 = (-1 + R_{12}^2 + R_{13}^2 + R_{23}^2 - 2R_{12}R_{13}R_{23})^2$ is the determinant of C and $J = \frac{1}{8}$ the Jacobian of the transformation from (A^r, A^i) to I.

To obtain the joint density of the intensities, we integrate on t and

$$\begin{aligned} &p(I_1, I_2, I_3) \\ &\quad = 2\pi \frac{|J|}{\Delta(2\pi)^3} \int_{-\pi}^{\pi}\int_{-\pi}^{\pi} dt dz e^{\frac{-I_1}{\Delta}(1-R_{23}^2)} e^{\frac{-I_2}{\Delta}(1-R_{13}^2)} e^{\frac{-I_3}{\Delta}(1-R_{12}^2)} \\ &\qquad \cdot e^{\frac{2}{\Delta}(R_{12}-R_{23}R_{13})\sqrt{I_1 I_2}\cos(t)} e^{\frac{2}{\Delta}(R_{13}-R_{12}R_{23})\sqrt{I_1 I_3}\cos(z)} e^{\frac{2}{\Delta}(R_{23}-R_{13}R_{12})\sqrt{I_2 I_3}\cos(z-t)} \end{aligned} \tag{28}$$

since $e^{z\cos t} = \sum_{k=0}^{\infty} \epsilon_k \mathcal{I}_k(z)\cos kt$ where $\epsilon_k = 1$ if $k = 0$ and $\epsilon_k = 2$ otherwise, we obtain

$$\begin{aligned} p(I_1, I_2, I_3) = \frac{1}{2\Delta}\exp\left\{\frac{-I_1}{\Delta}(1-R_{23}^2)\right\}\exp\left\{\frac{-I_2}{\Delta}(1-R_{13}^2)\right\}\exp\left\{\frac{-I_3}{\Delta}(1-R_{12}^2)\right\} \\ \cdot\left[\sum_{k=0,1,\ldots} \epsilon_k \mathcal{I}_k\left(-\frac{2}{\Delta}(R_{12}-R_{23}R_{13})\sqrt{I_1 I_2}\right)\mathcal{I}_k\left(-\frac{2}{\Delta}(R_{13}-R_{12}R_{23})\sqrt{I_1 I_3}\right)\right. \\ \left.\cdot\,\mathcal{I}_k\left(-\frac{2}{\Delta}(R_{23}-R_{13}R_{12})\sqrt{I_2 I_3}\right)\right]. \end{aligned} \tag{29}$$

Let us remark that the marginal densities I_j do not depend on j: $p(I_1) = p(I_2) = p(I_3)$ and $p(I_1) = \lambda e^{-\lambda I_1}$ with $\lambda = 1/2$, as expected, as these densities are derived from Gaussian

ones. Moreover

$$p(I_1, I_3) = \frac{1}{2}\frac{1}{2(1-R_{13})^2} e^{-\frac{1}{(1-R_{13}^2)}(I_1+I_3)} \mathcal{I}_0\left(\frac{R_{13}}{(1-R_{13}^2)}\sqrt{I_1 I_3}\right) \tag{30}$$

that is, the joint density of I_i and I_j, that does, as expected, not depend on i and j. Let $\underline{A} = \{A_1^r, A_1^i A_2^r, A_2^i, \ldots, A_n^r, A_n^i\}$ then

$$p(\underline{A}) = \frac{e^{-\frac{1}{2}(\underline{A})^t C^{-1}(\underline{A})}}{(2\pi)^n\sqrt{|C|}} \tag{31}$$

via the change of variables $A_j^r = \sqrt{I_j}\cos t_j$, $A_j^i = \sqrt{I_j}\sin t_j$, and if $\underline{\tilde{I}} = \{\sqrt{I_1}\cos t_1, \sqrt{I_1}\sin t_1, \ldots, \sqrt{I_n}\cos t_n, \sqrt{I_n}\sin t_n\}$ then

$$p(I_1, t_1, I_2, t_2, \ldots, I_n, t_n) = \frac{|J|}{(2\pi)^n\sqrt{|C|}} e^{-\frac{1}{2}(\underline{\tilde{I}})^t C^{-1}(\underline{\tilde{I}})} \tag{32}$$

where $|J|$ is the Jacobian of the transformation from (A^r, A^i) to I, t. Therefore

$$p(I_1, t_1, I_2, t_2, \ldots, I_n, t_n) = \frac{e^{-\frac{1}{2}\sum_{i=1}^n \lambda_i I_i} e^{2\sum_{i<j}\mu_{ij}\sqrt{I_i I_j}\cos(t_i - t_j)}}{(4\pi)^n\sqrt{|C|}}$$

where $\lambda_i I_i$ are the diagonal terms of $\tilde{I}^t C^{-1}\tilde{I}$ and $\mu_{ij}\sqrt{I_i I_j}\cos(t_i - t_j)$ are the $\frac{n(n-1)}{2}$ remaining terms. Integrating on $t_1, t_2, \ldots$ and expanding $e^{z\cos t} = \sum_{k=0}^{\infty}\epsilon_k \mathcal{I}_k(z)\cos kt$ we obtain

$$\begin{aligned} p(I_1, I_2, \ldots, I_n) = {} & \frac{1}{(4\pi)^n\sqrt{|C|}} e^{-\frac{1}{2}\sum_{i=1}^n \lambda_i I_i} \int_{-\pi}^{\pi}\ldots\int_{-\pi}^{\pi} dt_1 \ldots dt_n \\ & \cdot \sum_{k_1,\ldots,k_N} \epsilon_{k_1}\ldots\epsilon_{k_N}\mathcal{I}_{k_1}(2\mu_{12}\sqrt{I_1 I_2})\cos k_1(t_1 - t_2)\ldots \\ & \cdot \mathcal{I}_{k_N}(2\mu_{n-1,n}\sqrt{I_{n-1}I_n})\cos k_N(t_{n-1} - t_n) \end{aligned} \tag{33}$$

where $N = \frac{n(n-1)}{2}$. The integrals

$$\int_{-\pi}^{\pi}\ldots\int_{-\pi}^{\pi} dt_1 \ldots dt_n \cos k_1(t_1 - t_2)\ldots\cos k_N(t_{n-1} - t_n),$$

via the change of variables $t_1 - t_2 = x_1, \ldots, t_1 - t_n = x_n$, become

$$\int_{-\pi}^{\pi}\ldots\int_{-\pi}^{\pi} dt_1 \ldots dt_n \cos k_1 x_1 \ldots \cos k_n x_n \ldots \cos k_N(x_{n-1} - x_n).$$

For $n = 3$ only $k_1 = k_2 = k_3$ ($k_i \geq 0$) result in a non-zero integral. For $n \geq 4$, other combinations are possible, and we note these conditions by *, so that, in conclusion one obtains

$$\begin{aligned} & p(I_1, I_2, \ldots, I_n) \\ & = \frac{1}{(4\pi)^n\sqrt{|C|}} e^{-\frac{1}{2}\sum_{i=1}^n \lambda_i I_i}\mathcal{I}_0(\mu_{12}\sqrt{I_1 I_2})\ldots\mathcal{I}_0(\mu_{n-1,n}\sqrt{I_{n-1}I_n})(2\pi)^n \\ & \quad + (\pi)^n \sum_{k_1,\ldots,k_N,*,k_i\neq 0} \mathcal{I}_{k_1}(2\mu_{12}\sqrt{I_i I_j})\ldots\mathcal{I}_{k_N}(2\mu_{n-1,n}\sqrt{I_{n-1}I_n}). \end{aligned} \tag{34}$$

5 Decay of the Correlations

A numerical evaluation of the decrease of the off-diagonal terms of the inverse C^{-1} of the correlation matrix shows the decay $1/(|i-j|)^{\beta}$ with $\beta = 1$ in the z direction and $\beta = 3/2$ in the x direction, see Fig. 7. This is expected, as it is known [29] that if the elements $C_{i,2j-i}$ decrease as $1/(|i-j|)^{\alpha}$ (for $\alpha > 1$) then the elements of the inverse matrix decrease at the same speed. However, the numerical inversion is delicate, as small eigenvalues—which turn out to be the large ones in the inverse matrix—dominate the behaviour of the center of the inverse matrix, the center being the near-diagonal elements. The behaviour of the off-diagonal elements, which is of interest, is still dominated by the good eigenvalues, which gives the expected decay. This numerical investigation has the following theoretical counterpart: [30, 31] it is well-known from signal processing that the numerical inversion of covariance matrices, necessary to determine the probability density function, causes currently problems. A way to avoid these difficulties is to rely on the fact that properties of Toeplitz matrices can be applied. The inversion of such matrices has been abundantly investigated and common problems of matrix inversion can be avoided. Recall that the correlation matrix is $\int_0^{\kappa} k\cos(k^2 z)\mathcal{J}_0(kx)dk$. We shall deal with two Toeplitz hermitian matrices $T(x, z_0)$ and $T(x_0, z)$ which are the sections of the correlation matrix C in x and in z-direction, where

$$T(x,z) = \int_0^{\kappa} k\cos(k^2 z)\mathcal{J}_0(kx)dk \tag{35}$$

and their associated spectra

$$S_x(\lambda) = \int_0^{\infty} T(x,z_0)e^{-i\lambda x}dx \quad \text{and} \quad S_z(\lambda) = \int_{-\infty}^{\infty} T(x_0,z)e^{-i\lambda z}dz, \tag{36}$$

respectively. First considering $T(x, z_0 = 0)$, we have for the correlation and its transform:

$$T(x,0) = \kappa\frac{\mathcal{J}_1(\kappa x)}{x}, \qquad S_x(\lambda) = \int_{-\infty}^{\infty} e^{-i\lambda x}\kappa\frac{\mathcal{J}_1(\kappa x)}{x}dx = \kappa\sqrt{1-(\lambda/\kappa)^2} \tag{37}$$

for $|\lambda| \le \kappa$. Following Grenander and Szegö [30], we start with the function $S_x(\lambda) = \kappa\sqrt{1-(\lambda/\kappa)^2}$ defined on the interval $[-\kappa, \kappa]$ and the Toeplitz matrix associated to S, e.g.

$$(\mathcal{M}_n)_{\mu\nu} = \int_{-\kappa}^{\kappa}\sqrt{1-(x/\kappa)^2}e^{i(\nu-\mu)x}dx = \frac{\pi\mathcal{J}_1(\kappa(\nu-\mu)}{(\nu-\mu)}.$$

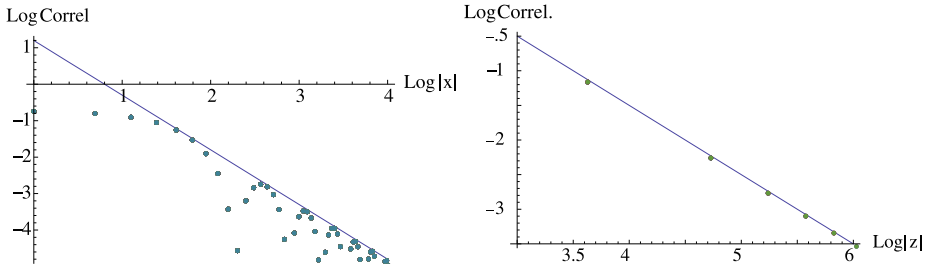

Fig. 7 Decrease of correlation in x (*left*) and z (*right*). *Each dot* indicates the value of an element of the correlation matrix with respect to the distance between the two points for which the correlation has been computed. *Solid line*: scaling law with $x^{-3/2}$, and z^{-1}, respectively

We take (see [30]) the following sequence approximating the spectrum S, with a Cesaro sum applying a linear decrease $1 - |n|/p$:

$$S_{p,x}(\lambda) = \sum_{n=-p}^{p} (1 - |n|/p) c_n e^{-in\lambda} \tag{38}$$

with Fourier coefficients $c_n = \mathcal{J}_1(\kappa n)/2n$ and $c_0 = \kappa/4$. We define as in [30] the diagonal matrix $(D_n)_{\nu\nu} = S_{p,x}(2\pi\nu/n)$ and the matrix

$$(L_n)_{\nu\mu} = \frac{1}{n} \sum_{m=1}^{n} S_{p,x}(2\pi m/n) e^{im\frac{(\nu-\mu)}{n}}. \tag{39}$$

The latter, L_n, is a circulant matrix whose eigenvalues are $S_{p,x}(2\pi\nu/n)$ and we know that for a circulant matrix associated to S, $(L_n(S))^{-1} = L_n(1/S)$ so that [31]

$$(L_n)^{-1}_{\nu\mu} = \frac{1}{n} \sum_{m=1}^{n} \frac{e^{im(\nu-\mu)/n}}{S_{p,x}(2\pi m/n)}. \tag{40}$$

L_n is asymptotically equivalent to the Toeplitz matrix $\mathcal{M}_n$ [30, 31].

This choice of approximating sequences $S_{p,x}$ (convolutions) allows to handle the case of a convergent, but not absolutely convergent Fourier series [30]. This is indeed the case in the z direction, when $\alpha = 1$. Moreover, in the discretisation of S_p, we keep away from generate large eigenvalues for L_n^{-1} so that L_n^{-1} is asymptotically equivalent to the inverse $\mathcal{M}_n^{-1}$ of the Toeplitz matrix $\mathcal{M}_n$ [31].

Taking $S_{p,x}$ as in (38), with the coefficients c_n, we have for $T^{-1}(x, s)$, $s = \mu - \nu$:

$$T^{-1}(x, s) \sim \frac{1}{n} \sum_{m=1}^{n} \frac{e^{im\, s/n}}{S_{p,x}(2\pi m/n)}, \tag{41}$$

which gives, for large n and s values ($s \leq n$) the decay of the off-diagonal elements of the inverse matrix.

We have examined the decrease numerically starting from a covariance matrix and evaluated the decrease in the inverse matrix by applying the procedure shown above, using Cesaro sums. The numerical evaluation of the above-mentioned expression confirms indeed the decay as $\sim s^{-3/2}$, see Fig. 8 (left). In the same way, for $T(x_0 = 0, z)$ in the z section, we have

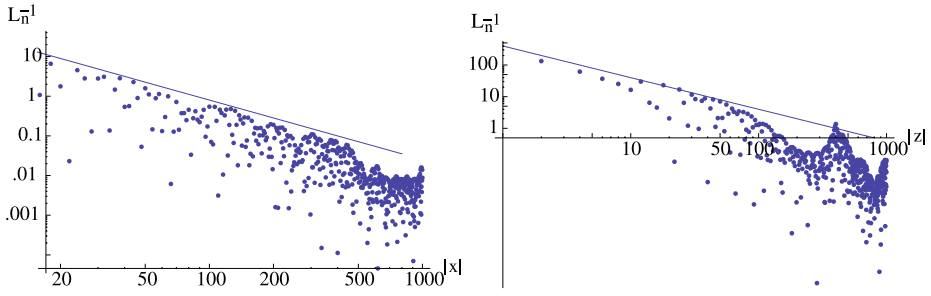

Fig. 8 Decrease of correlation in x (*left*) and in z (*right*) in the inverse Matrix, reconstructed via a Toeplitz Matrix, *solid line*: scaling law with $x^{-3/2}$ and with z^{-1}, respectively

for $x_0 = 0$ the correlation and its transform given by:

$$T(0,z) = \begin{cases} \frac{\sin(z\kappa^2)}{z} & \text{if } z \neq 0, \\ \frac{\kappa^2}{2} & \text{otherwise,} \end{cases} \tag{42}$$

$$S_z(\lambda) = 2\int_0^\infty \frac{\sin(x\kappa^2)}{x}\cos(\lambda x)dx = \begin{cases} 1 & \text{if } |\lambda| < \kappa^2, \\ 0 & \text{if } |\lambda| > \kappa^2. \end{cases} \tag{43}$$

We repeat the same approximating procedure as above, (38)–(41), taking as the sequence approximating the spectrum $S_{p,z}(\lambda) = \sum_{n=-p}^{p}(1-|n|/p)c_n \exp\{-in\lambda\}$, where the Fourier coefficients are given by $c_n = \sin(\kappa^2 n)/\pi n$ and $c_0 = \kappa^2/\pi$.

We define as in [30] the diagonal matrix $(D_n)_{\nu\nu} = S_{p,z}(2\pi\nu/n)$ and the matrix $(L_n)_{\nu\mu} = (1/n)\sum_{m=1}^{n} S_{p,z}(2\pi m/n)\exp\{im(\nu-\mu)/n\}$, where, again, L_n is a circulant matrix whose eigenvalues are $S_{p,z}(2\pi\nu/n)$, for which know that for the circulant matrix associated with S $(L_n(S))^{-1} = L_n(1/S)$ so that [31] $(L_n)^{-1}_{\nu,\mu} = (1/n)\sum_{m=1}^{n}\exp\{im(\nu-\mu)/n\}/S_{p,z}(2\pi m/n)$. We find for the decay of the inverse Toeplitz Matrix, with $\nu - \mu = s$,

$$T^{-1}(s,z) \sim \frac{1}{n}\sum_{m=1}^{n}\frac{e^{im\,s/n}}{S_{p,z}(2\pi m/n)}. \tag{44}$$

We have again examined the decrease numerically and evaluated it by applying the procedure equivalent to what was shown above. The numerical evaluation of the above expression gives indeed a decay $\sim s^{-1}$, see Fig. 8 (right).

6 The Total Intensity

We discuss the behaviour of the total intensity $S_n = I_1 + \cdots + I_n$ of a speckle pattern evaluated at n points. This is of importance to estimate the weight of the maximum of the sequence, M_n, with respect of the ensemble. As the total intensity S_n is the sum of n weakly correlated variables I_j, $j = 1, \ldots, n$, all following the exponential law with parameter $\lambda = 1/2$, let us consider $S_n = I_1 + \cdots + I_n$ and note that the sequence $I_1, \ldots, I_n$ satisfies the following mixing property:

For any sequence of indices $1 < i_1 < \cdots < i_k$, $i_k + n < j_1 < \cdots < j_t$, for any sequence of real values $u_{i_1}, \ldots, u_{i_k}, u_{j_1}, \ldots, u_{j_t}$ it holds that

$$\begin{aligned} &|P(I_{i_1} < u_{i_1}, \ldots, I_{i_k} < u_{i_k}, I_{j_1} < u_{j_1}, \ldots, I_{j_t} < u_{j_t}) \\ &\quad - P(I_{i_1} < u_{i_1}, \ldots, I_{i_k} < u_{i_k})P(I_{j_1} < u_{j_1}, \ldots, I_{j_t} < u_{j_t})| \leq \alpha(n), \end{aligned} \tag{45}$$

where $\alpha(n) \to 0$ as $n \to \infty$: the coefficients $\alpha(n)$ decrease to 0 as μ^2_{1n}, that is as $(1/n)^a$ $(a = 2)$, see Sect. 5. For a proof, see Appendix C.

Moreover, the sequence $\{I_i\}_{i=1,2,\ldots}$ of weakly correlated exponential variables of parameter $\lambda = 1/2$ satisfies the condition on the upper tail quantile function $Q(u) \doteq \inf\{t : P(I > t) \leq u\} = \inf\{t : \int_t^\infty \lambda e^{-\lambda t}dt \leq u\} = \frac{-1}{\lambda}\log u$:

$$\sum_{n=1}^{\infty}\int_0^{\alpha(n)} Q^2(u)du < \infty.$$

Furthermore, we know that (see [32]), $\lim_{n\to\infty} \mathrm{Var}(S_n)/n = \sigma^2 \in \mathbb{R}_*^+$ where $\mathrm{Var}(S_n)$ denotes the variance of the random variable S_n. We can apply the Central Limit Theorem (CLT) saying that the law $\mathcal{L}$

$$\mathcal{L}\left(\frac{I_1 + \cdots + I_n - E(S_n)}{\sigma\sqrt{n}}\right) \to \mathcal{N}(0,1),$$

where $E()$ and $\mathcal{N}$ stand for the expectation value and the normal (Gaussian) distribution, respectively, and, here, $E(S_n) = nE(I) = n/\lambda$ the expectation value of the total intensity. Note that it can be directly checked that $(1/n)\mathrm{Var}(I_1 + \cdots + I_n)$ converges toward a finite and positive quantity. Computing the variance $\mathrm{Var}(S_n) = \sum_i \mathrm{Var}(I_i) + 2\sum_{1\le i<j\le n} \mathrm{Cov}(I_i I_j)$ where $\mathrm{Var}(I_j) = 1/\lambda^2 \equiv 4$ with $\lambda = 1/2$, and the covariances are $\mathrm{Cov}(I_i I_j) = E(I_i I_j) - E(I_i)E(I_j)$ yields

$$E(I_i I_j) = \int_0^\infty \int_0^\infty \frac{1}{2}\,\frac{I_i I_j}{2(1-\mu_{ij}^2)} e^{\frac{-1}{2}\frac{(I_i+I_j)}{1-\mu_{ij}^2}} \mathcal{I}_0(\mu_{ij}\sqrt{I_1 I_j}) dI_i dI_j = 4(1+\mu_{ij}^2) \tag{46}$$

having used $2\int_0^\infty ay\exp(-ay)\int_0^\infty x^3\exp(-ax^2)\mathcal{I}_0(b\sqrt{y}\,x)dxdy = 16a(4a^2+b^2)/(4a^2-b^2)^3$, with $a = 1/2(1-\mu_{ij}^2)$ and $b = \mu_{ij}$. Hence,

$$\begin{aligned}\mathrm{Var}(S_n) &= n\frac{1}{\lambda^2} + 2\sum_{1\le i<j\le n}\left(E(I_i I_j) - \frac{1}{\lambda^2}\right)\\ &= \frac{n}{\lambda^2} + 2\sum_{1\le i<j\le n}\left(4(1+\mu_{ij}^2) - \frac{1}{\lambda^2}\right) = \frac{n}{\lambda^2} + 8\sum_{1\le i<j\le n}\mu_{ij}^2.\end{aligned} \tag{47}$$

To show the convergence of the last series, recall that correlations decrease with power laws, $\mu_{ij} \sim |i-j|^{-D}$ with $D = 1$ and $D = 3/2$, respectively, if $|i-j| = k$ is large, say $k \ge k_0$. Hence the variance can be estimated for $\lambda = 1/2$ by

$$\mathrm{Var}(S_n) \sim 4n + 8\left(c(n) + \sum_{k=k_0}^{n}\frac{(n-k)}{k^{2D}}\right),$$

where $\sum_{k=k_0}^n \frac{(n-k)}{k^2}$ grows, for $D = 1$ as $n - \log n - 1$ and for $D = 3/2$ as $\sum_{k=k_0}^n \frac{(n-k)}{k^3}$ as $n/2 + 1/2n - 1$, and $c(n) \le \sqrt{n}$, showing the convergence toward a finite and positive limit, denoted by σ^2, of $(1/n)\,\mathrm{Var}(I_1 + \cdots + I_n)$ when $n \to \infty$.

Observe that (see [9, 10]) the total intensity $S_n = I_1 + \cdots + I_n = \sum_j |A_j|^2 = \sum_j (|A'_j|)^2 = I'_1 + \cdots + I'_n$, is invariant with respect to the transformation where the variables $A' = PA$ are the transformed by an unitary matrix P variables. The total intensity is hence the same in the original and transformed basis. Hence we can describe S_n as the sum of n independent variables I'_j, where I'_j follows the exponential law:

$$p(I'_j) = \lambda_j e^{-\lambda_j I'_j}\chi_{[0,\infty]}(I'_j),$$

with $\chi_{[0,\infty]}(I'_j) = 1$ for $I'_j \ge 0$, and 0 elsewhere, and where λ_j is the inverse of the j-th eigenvalue of the correlation matrix. Since the I'_k are uncorrelated, the characteristic function

of the total intensity S_n is: $\phi_{S_n}(t) = \prod_{k=1}^{n} \frac{\lambda_k}{\lambda_k - it}$ and its Fourier transform

$$p_{S_n}(x) = \sum_{k=1}^{n} \frac{e^{-x\lambda_k} \lambda_1 \cdots \lambda_n}{\prod_{p \neq k} (\lambda_p - \lambda_k)} \tag{48}$$

is the probability density function of S_n (as all λ_k are different from each other) [9, 10].

For $S_n = I_1 + \cdots + I_n = I'_1 + \cdots + I'_n$, and for small n, the total intensity S_n as sum of exponential variables, is dominated by the term associated to the smallest λ_k (see Fig. 9).

The contribution of the maximum term corresponding to the sequence $(I_i)_{i \in N}$, represented by the quantity M_n, is asymptotically negligible with respect to the total intensity S_n:

$$\frac{M_n}{S_n} \to 0 \tag{49}$$

due to its exponential distribution [21]. Furthermore, as the I_i are weakly correlated and S_n is asymptotically Gaussian, the individual terms will be asymptotically negligible and the extreme terms play no role in the limit distribution, that is to say we expect the asymptotic independence of S_n and M_n [33]. In Fig. 10 is shown the behaviour of M_n/S_n confirming that the contribution of the maximum term to the sum, for the case discussed here, is asymptotically negligible.

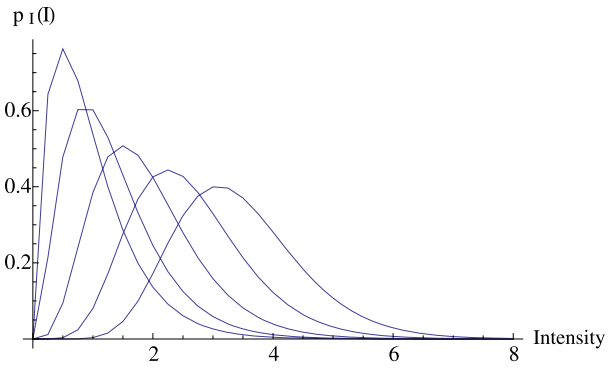

Fig. 9 Probability density function of total intensity for a sum of a speckle pattern discretized over 12×12 points, retaining 2, 5, 8, and 12 eigen values (from the *left* to the *right*). With increasing number of eigen values, the shape approaches a normal (Gaussian) law

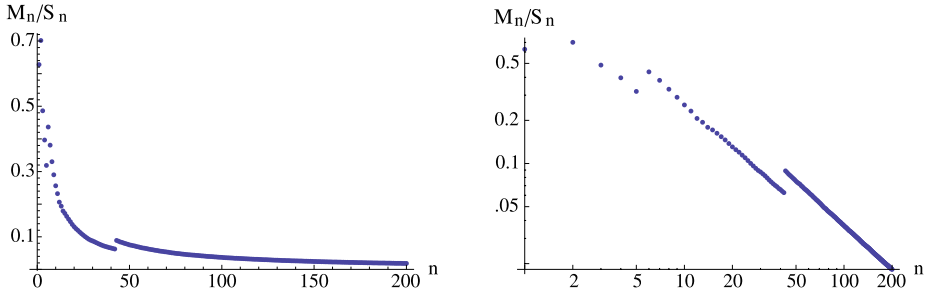

Fig. 10 Ratio relating the sum over intensity extrema M_n to the sum of all field values S_n computed successively from n from 1 to all 200, clearly showing the decrease of $S_n/M_n \sim 1/n \to 0$ for $n \to \infty$. *Left*: linear scale, *right*: log-log scale

7 The General Model

In the previous sections we have considered the case $C^{ir} = -C^{ri} = 0$. For completeness, we consider now the general case $C^{ir} = -C^{ri} \neq 0$ for a circular complex random variable (see [9, 10]). The proofs are technically heavier but it is important to note that it follows the same lines that in the simpler $C^{ir} = -C^{ri} = 0$. We proceed as in Sect. 4.1

7.1 The Model for $n = 2$

$$C = \begin{pmatrix} \sigma^2 & 0 & \mu & \delta \\ 0 & \sigma^2 & -\delta & \mu \\ \mu & -\delta & \sigma^2 & 0 \\ \delta & \mu & 0 & \sigma^2 \end{pmatrix}. \tag{50}$$

With $\sigma^2 = 1$, one obtains $\operatorname{Det} C = (-1 + \delta^2 + \mu^2)^2$, and for the joint density

$$p(I_1, I_2, t_1, t_2) = \frac{1}{2\pi(-1+\delta^2+\mu^2)} e^{\frac{-1}{2}\frac{1}{1-\delta^2-\mu^2}(I_1+I_2-2\mu\sqrt{I_1 I_2}\cos(t_1-t_2)+2\delta\sqrt{I_1 I_2}\sin(t_1-t_2))}$$

so that the joint density of the intensities only yields

$$p(I_1, I_2) = \frac{4\pi}{(-1+\delta^2+\mu^2)} e^{\frac{-1}{2}\frac{1}{1-\delta^2-\mu^2}(I_1+I_2)} \mathcal{I}_0\left(\frac{\sqrt{\mu^2+\delta^2}}{(-1+\delta^2+\mu^2)} 2\sqrt{I_1 I_2}\right).$$

Note that as $\mu, \delta \to 0$ the joint density tends towards the product of densities.

7.2 The Model for $n = 3$

Setting $\sigma^2 = 1$, and observing that the terms containing a sinus vanish (for $n = 3$) we have the joint density:

$$p(I_1, I_2, I_3, t_1, t_2, t_3) = \frac{e^{\frac{-1}{2}(\delta_1 I_1 + \delta_2 I_2 + \delta_3 I_3)}}{(4\pi)^3\sqrt{\det|C|}} e^{\mu_{12}\cos(t_1-t_2)+\mu_{13}\cos(t_1-t_3)+\mu_{23}\cos(t_2-t_3)}$$

and proceeding as above (see §1.2) the joint density of the intensities:

$$p(I_1, I_2, I_3) = \frac{e^{-\frac{1}{2}(\delta_1 I_1 + \delta_2 I_2 + \delta_3 I_3)}}{(4\pi)^3\sqrt{\det|C|}} \left(8\pi^3 \sum_k \epsilon_k \mathcal{I}_k(\mu_{12}\sqrt{I_1 I_2})\mathcal{I}_k(\mu_{13}\sqrt{I_1 I_3})\mathcal{I}_k(\mu_{23}\sqrt{I_2 I_3})\right). \tag{51}$$

The latter is easy to generalise to n variables.

7.3 The General Case n

The covariance matrix has the form

$$C = \begin{pmatrix} 1 & 0 & R_{12} & L_{12} & R_{13} & L_{13} & \dots \\ 0 & 1 & -L_{12} & R_{12} & -L_{13} & R_{13} & \dots \\ R_{12} & -L_{12} & 1 & 0 & R_{23} & L_{23} & \dots \\ L_{12} & R_{12} & 0 & 1 & -L_{23} & R_{23} & \dots \\ R_{13} & -L_{13} & R_{23} & -L_{23} & 1 & 0 & \\ L_{13} & R_{13} & L_{23} & R_{23} & 0 & 1 & \dots \\ \dots & & & & & & \end{pmatrix}. \tag{52}$$

Hence, proceeding as above, we find

$$p(I_1,t_1,I_2,t_2,\ldots,I_n,t_n)=\frac{e^{-\frac{1}{2}\sum_{i=1}^{n}\lambda_i I_i}}{(4\pi)^n\sqrt{|C|}}e^{2\sum_{i<j}\mu_{ij}\sqrt{I_iI_j}\cos(t_i-t_j)}e^{2\sum_{i<j}\lambda_{ij}\sqrt{I_iI_j}\sin(t_i-t_j)} \quad (53)$$

where μ_{ij} are the coefficients of C^{-1} correlating real to real or complex to complex, and λ_{ij} those relating complex to real (or real to complex). These coefficients decay to *zero* when $i-j$ is large at a rate which can be inferred by that of the off-diagonal coefficients of the matrix C, as above. By using the expansions $e^{z\cos t}=\sum_{k=0}^{\infty}\epsilon_k\mathcal{I}_k(z)\cos(kt)$ and $e^{z\sin t}=\mathcal{I}_0(z)+2\sum_{k=0}^{\infty}(-1)^k\mathcal{I}_{2k+1}(z)\sin((2k+1)t)+2\sum_{k=0}^{\infty}(-1)^k\mathcal{I}_{2k}(z)\cos(2kt)$ we obtain

$$\begin{aligned}
&p(I_1,I_2,\ldots,I_n)\\
&\quad=\frac{e^{-\frac{1}{2}\sum_{i=1}^{n}\lambda_i I_i}}{(4\pi)^n\sqrt{|C|}}\int_{-\pi}^{\pi}\ldots\int_{-\pi}^{\pi}dt_1\ldots dt_n\\
&\qquad\cdot\Bigg[\sum_{k_1,\ldots,k_N}\epsilon_{k_1}\ldots\epsilon_{k_N}\mathcal{I}_{k_1}(r_{12}\sqrt{I_1I_2})\ldots\mathcal{I}_{k_N}(r_{n-1,n}\sqrt{I_{n-1}I_n})\\
&\qquad\cdot\cos(k_1(t_1-t_2))\ldots\cos(k_n(t_1-t_n))\ldots\cos(k_N(t_n-t_{n-1}))\Bigg]\\
&\qquad\cdot\Bigg[\prod_{i\neq j}\mathcal{I}_0(\lambda_{ij}\sqrt{I_iI_j})+2\sum_{k_i}(-1)^{k_i}\mathcal{I}_{2K_i+1}(\lambda_{ij}\sqrt{I_iI_j})\sin(2K_i+1)(t_i-t_j)\\
&\qquad+2\sum_{k_i}(-1)^{k_i}\mathcal{I}_{2K_i}(\lambda_{ij}\sqrt{I_iI_j})\cos(2K_i)(t_i-t_j)\Bigg] \qquad (54)
\end{aligned}$$

hence

$$\begin{aligned}
&p(I_1,I_2,\ldots,I_n)\\
&\quad=\frac{e^{-\frac{1}{2}\sum_{i=1}^{n}\lambda_i I_i}}{(4\pi)^n\sqrt{|C|}}\Bigg[(\mathcal{I}_0(r_{12}\sqrt{I_1I_2})\ldots\\
&\qquad\cdot\mathcal{I}_0(r_{n-1,n}\sqrt{I_{n-1}I_n}))\cdot(\mathcal{I}_0(l_{12}\sqrt{I_1I_2})\ldots\mathcal{I}_0(l_{n-1,n}\sqrt{I_{n-1}I_n}))+\sum\prod\Bigg]. \qquad (55)
\end{aligned}$$

As μ_{ij} and λ_{ij} go to zero, the terms $\sum\prod$ go to zero faster than the product of the zero order modified Bessel function $\mathcal{I}_0$'s. The proof proceeds as shown above.

8 Conclusions and Discussion

We have shown that the extremal properties of the speckle statistics yield a Gumbel law for the probability distribution of the maximum of a sequence of n intensity values measured inside a speckle pattern. The probability for the maximum of this sequence of intensity values (normalized to the mean intensity), given by

$$P(\max(I_1,\ldots,I_n<u)=H^{\theta}(u-\log n)=\exp-\theta e^{-(u-\log n)}$$

is centered around the (normalized) intensity $u=\log n/\theta$ (equivalent to $u=\log n$ for $\theta\equiv 1$ when all points are uncorrelated).

For the limit of a highly resolved speckle pattern, where the number of points resolved n is much higher than the number of potential speckles n_{sp} in the pattern, $n \gg n_{\mathrm{sp}}$, the maximum of the measured values follows as well a Gumbel law with a θ-value $\theta \simeq n_{\mathrm{sp}}/n \ll 1$. This law asymptotically, for $n/n_{\mathrm{sp}} \gg 1$, converges toward a distribution centered around the (normalized) intensity $u \simeq \log n_{\mathrm{sp}}$, and being equivalent to the distribution for the *principal intensity maximum* of the speckle pattern, the probability density of which is given by (18). The latter convergence is due to the presence of clusters inside the coherent structure of a speckle, which yields an upper limit for the number of independent points n on which the field pattern can be measured, given by the number of speckles n_{sp} in the considered volume. The fact that the distributions of sequences with an increasing number of points converge to a unique distribution once n is much higher than the number of potential speckles in the pattern, demonstrates the robustness of our finding.

Our work is distinct form previous work [11, 19, 20] in that we use an approach starting from the Gumbel law as the extremal value distribution. The form of the extremal law in our approach is exact. The only approximation made was in the analytical expression for the parameter θ, developed up to the 2nd order in the correlations of clustering (Appendix B.1); in parallel to this, we have found an approximate expression for θ derived from numerical simulations. It is important to mention that both the analytic expression and the numerically found expression recover the essential scaling of θ on the characteristic speckle sizes, determining eventually the number of speckles n_{sp} in the pattern. Numerical constants which may change along with the precision of the development, are of minor importance due to the logarithmic dependence of the distribution on n_{sp}.

Our findings are of essential importance for processes where the most intense speckles contribute considerably (see e.g. [4]) or even critically to a process (see e.g. [1, 34]), mostly of nonlinear nature, such as signal amplification as a function of the light intensity.

It is also of interest if one tries to model a speckle distribution with realisations of a relatively small number of speckles. As an example we mention the often used restriction to two spatial (2D) dimensions instead of three dimensions (3D). A 2D case represents obviously only one slice of a 3D case: supposing that the third dimension of the speckle pattern has an extension of D and a is the radius of a single speckle, a 3D case would correspond to a number of $D/2a$ realisations, where usually $D/2a \gg 1$ holds.

Our findings allow to determine the error in the expected observations of the peak intensity of the speckle pattern. The interval of intensity values in which the most intense speckles will occur can be characterized by lower and an upper bound in intensity. It is important to note that the intensity value associated with the lower bound characterizing the Gumbel distribution, see (18), exhibits a sharp onset as a function of the intensity, while the upper tail of the distribution decreases quite smoothly with intensity. The latter is of importance in particular for nonlinear processes, as amplification of parametric instabilities in laser plasmas, because an amplification growing exponentially with the intensity can overcome the decrease of the probability density in the intensity tail. The weight of the intense speckles (not only of the most intense one), which is negligible when compared to the total intensity, see Sect. 6, can therefore have considerable importance, as e.g. underlined in [1, 34].

The feature of a sharp onset for the lower bound, of the interval in which the most intense speckle (the *principal intensity maximum*) can be found, is directly connected with the order statistics of the next speckle intensity maxima in hierarchy. It is also characteristic for the considered case, namely a marginal probability density for speckle patterns that can be described by an exponential law [see (25)], $\propto \exp(-\lambda u)$, with a single characteristic exponent λ standing for the average intensity of the speckle pattern. The latter is not the case for composed probability densities that cannot be characterized by a single λ value. These subjects are actually work in progress.

Acknowledgements We wish to thank Ph. Mounaix for helpful discussions. This work has been partially supported by the Agence Nationale de Recherche, project title "CORPARIN" no. ANR-07-BLAN-0004. Simulations have been performed thanks to access to the computing center IDRIS-CNRS.

Appendix A: Proof of Condition 1

First we prove that the d.f. F with density p is mixing in the upper tail, that is, it satisfies the following:

$$|P(I_{i_1} < u, \ldots, I_{i_k} < u, I_{j_1} < u, \ldots, I_{j_t} < u) - P(I_{i_1} < u, \ldots, I_{i_k} < u)P(I_{j_1} < u, \ldots, I_{j_t} < u)| \leq \tau(s, u)$$

where $1 < i_1 < \cdots < i_k$, $i_k + s < j_1 < \cdots < j_t$ and $\tau(s, u)$ is non increasing in u and such that for at least a sequence $u_n \to \infty$ there exists a sequence $s_n \to \infty$ such that $\tau(s_n, u_n) \to 0$ when $n \to \infty$. We suppose that the correlations decrease with the mutual distance like $\mu_{ij} \leq |i - j|^{-\alpha}$ if $|i - j| > s$. This yields, by writing sums over products of higher order Bessel function symbolically, $\sum\prod \mathcal{I}_{k_l}(\ldots)$,

$$\begin{aligned}
&|P(I_{i_1} < u, \ldots, I_{i_k} < u, I_{j_1} < u, \ldots, I_{j_t} < u) \\
&\quad - P(I_{i_1} < u, \ldots, I_{i_k} < u) \cdot P(I_{j_1} < u, \ldots, I_{j_t} < u)| \\
&\leq \left| \int_0^u \cdots \int_0^u e^{-\frac{1}{2}\sum_{i=1}^{k+t}\lambda_i I_i} \Bigg(\prod_{(i,j),\binom{k+t}{2}\text{ terms}} \mathcal{I}_0(\mu_{ij}\sqrt{I_i I_j}) + \sum\prod \mathcal{I}_{k_l}(\ldots) \Bigg) dI_1 \ldots dI_k \ldots dI_t \right. \\
&\quad - \int_0^u \cdots \int_0^u e^{-\frac{1}{2}\sum_{i=1}^{k}\lambda_i I_i} \Bigg(\prod_{(i,j),\binom{k}{2}\text{ terms}} \mathcal{I}_0(\mu_{ij}\sqrt{I_i I_j}) + \sum\prod \mathcal{I}_{k_l}(\ldots) \Bigg) dI_1 \ldots dI_k \\
&\quad \left. \cdot \int_0^u \cdots \int_0^u e^{-\frac{1}{2}\sum_{i=1}^{t}\lambda_i I_i} \Bigg(\prod_{(i,j),\binom{t}{2}\text{ terms}} \mathcal{I}_0(\mu_{ij}\sqrt{I_i I_j}) + \sum\prod \mathcal{I}_{k_l}(\ldots) \Bigg) dI_1 \ldots dI_t \right| . \qquad (56)
\end{aligned}$$

Since $i_k + s < j_1$, the arguments $\mu_{ij}\sqrt{I_j I_j}$ of the Bessel functions decrease, at $I_i I_j$ fixed, as $|i - j|^{-\alpha} \leq s^{-\alpha}$. As $\binom{k+t}{2} = \binom{k}{2} + \binom{t}{2} + \binom{k}{1}\binom{t}{1}$ i.e. correlations split into first block, second block, and between blocks (separated by s) correlations:

$$\begin{aligned}
&\leq \left| \int_0^u \cdots \int_0^u dI_1 \ldots dI_k \ldots dI_t \ldots \right. \\
&\quad \cdot \Bigg(\prod_{(i,j),\binom{k}{2}\text{ terms}} \mathcal{I}_0(\mu_{ij}\sqrt{I_i I_j}) + \sum\prod \mathcal{I}_{k_l}(\ldots) \Bigg) e^{-\frac{1}{2}\sum_{i=1}^{k}\lambda_i I_i} \\
&\quad \cdot \Bigg(\prod_{(i,j),\binom{t}{2}\text{ terms}} \mathcal{I}_0(\mu_{ij}\sqrt{I_i I_j}) + \sum\prod \mathcal{I}_{k_l}(\ldots) \Bigg) e^{-\frac{1}{2}\sum_{i=1}^{t}\lambda_i I_i} \\
&\quad \left. \cdot \Bigg(\prod_{(i,j),\binom{k}{1}\binom{t}{1}\text{ terms}} \mathcal{I}_0(\mu_{ij}\sqrt{I_i I_j}) + \sum\prod \mathcal{I}_{k_l}(\ldots) \Bigg) \right.
\end{aligned}$$

$$-\int_0^u \dots \int_0^u dI_1 \dots dI_k e^{-\frac{1}{2}\sum_{i=1}^k \lambda_i I_i} \Bigg(\prod_{(i,j),\binom{k}{2}\text{ terms}} \mathcal{I}_0(\mu_{ij}\sqrt{I_i I_j}) + \sum \prod \mathcal{I}_{k_l}(\dots) \Bigg)$$

$$\cdot \int_0^u \dots \int_0^u dI_1 \dots dI_t e^{-\frac{1}{2}\sum_{i=1}^t \lambda_i I_i} \Bigg(\prod_{(i,j),\binom{t}{2}\text{ terms}} \mathcal{I}_0(\mu_{ij}\sqrt{I_i I_j}) + \sum \prod \mathcal{I}_{k_l}(\dots) \Bigg) \Bigg| \tag{57}$$

where the term $\sum \prod \mathcal{I}_{k_l}(\dots)$ involves, again, the sum over products of Bessel functions $\mathcal{I}_i$ of order higher than 0. This difference can be estimated as

$$\begin{aligned} &\le \int_0^u \dots \int_0^u dI_1 \dots dI_k \dots dI_t e^{-\frac{1}{2}\sum_{i=1}^k \lambda_i I_i} e^{-\frac{1}{2}\sum_{i=1}^t \lambda_i I_i} \\ &\cdot \Bigg(\prod_{(i,j),(k)(k-1)/2\,\text{terms}} \mathcal{I}_0(\mu_{ij}\sqrt{I_i I_j}) + \sum \prod \mathcal{I}_{k_l}(\dots) \Bigg) \\ &\cdot \Bigg(\prod_{(i,j),(t)(t-1)/2\,\text{terms}} \mathcal{I}_0(\mu_{ij}\sqrt{I_i I_j}) + \sum \prod \mathcal{I}_{k_l}(\dots) \Bigg) \\ &\cdot \Bigg| \prod_{(i,j),kt\,\text{terms}} \mathcal{I}_0(\mu_{ij}\sqrt{I_i I_j}) + \sum \prod \mathcal{I}_{k_l}(\dots) - 1 \Bigg|. \end{aligned} \tag{58}$$

Since in the last product only block-block correlations between blocks separated by s are involved, we have $\mu_{ij} \le s^{-\alpha}$ and $\mathcal{I}_0(\mu_{ij}\sqrt{I_i I_j}) \le \mathcal{I}_0(u/s^\alpha)$. We choose the sequence u_n as $u_n = \log n$ and s_n such that $s_n/n \to 0$ an $n \to \infty$. We then find $\mathcal{I}_0(u/s^\alpha) \to 1$, for $\alpha > 0$, as $n \to \infty$ and $\sum \prod \mathcal{I}_{k_l} \to 0$ as $n \to \infty$, where we have used that for z small $\mathcal{I}_0(z) - 1 \sim z^2/4$ and $I_n(z) \sim (z/2)^n \Gamma(n+1)$.

Appendix B: Proof of Condition 2

Let $n = NM$, with $N \in \mathbb{N}^*$, $M \in \mathbb{N}^*$. The condition for the "non-clustering" property for the sequence $I_1, \dots, I_n$ reads:

$$\limsup_{N\to\infty} N \sum_{j=2}^N P(I_1 > u_{NM}, I_j > u_{NM}) = o\left(\frac{1}{M}\right) \tag{59}$$

as $M \to \infty$. We proceed in analyzing the non-clustering property.

$$\begin{aligned} &\limsup_{N\to\infty} N \sum_{j=2}^N P(I_1 > u_{NM}, I_j > u_{NM}) \\ &= \limsup_{N\to\infty} N \sum_{j=2}^N \int_{u_{NM}}^\infty \int_{u_{NM}}^\infty \frac{1}{2} e^{-\frac{1}{2}\frac{(I_1+I_j)}{1-\mu_{1j}^2}} \mathcal{I}_0\left(\frac{\mu_{1j}}{1-\mu_{1j}^2}\sqrt{I_1 I_j}\right) dI_1 dI_j. \end{aligned} \tag{60}$$

The coefficient μ_{1j} is the correlation coefficient between P_1 and P_j. We split the sum in two parts: the first one, on the terms involving the points sufficiently close to P_1 to have a significant correlation with it, and the other, say starting from an index $\bar{j}$, for which the correlation with P_1 can be estimated as to be smaller than $1/s^\alpha$.

In the first sum we use the expansion for z large: $\mathcal{I}_0(z) = \frac{e^z}{\sqrt{2\pi z}}(1 + \frac{1}{8z} + O(\frac{1}{z^2}))$. In the second one, we use the expansion for z small: $\mathcal{I}_0(z) = 1 + \frac{z^2}{4} + O(z^4)$.

By denoting the integral kernel as

$$\mathcal{K}(I_1, I_j) = e^{-\frac{1}{2}\frac{(I_1+I_j)}{1-\mu_{1j}^2}}\mathcal{I}_0\left(\frac{\mu_{1j}}{1-\mu_{1j}^2}\sqrt{I_1 I_j}\right),$$

we have

$$N\sum_{j=2}^{N}\int_{u_{NM}}^{\infty}\int_{u_{NM}}^{\infty}\mathcal{K}(I_1, I_j)dI_1 dI_j$$

$$= N\sum_{j=2}^{\bar{j}}\int_{u_{NM}}^{\infty}\int_{u_{NM}}^{\infty}\mathcal{K}(I_1, I_j)dI_1 dI_j + \sum_{j=\bar{j}}^{N}\int_{u_{NM}}^{\infty}\int_{u_{NM}}^{\infty}\mathcal{K}(I_1, I_j)dI_1 dI_j.$$

For a first estimate, let us consider the second sum

$$N\sum_{j=\bar{j}}^{N}\int_{u_{NM}}^{\infty}\int_{u_{NM}}^{\infty}e^{-\frac{1}{2}\frac{(I_1+I_j)}{1-\mu_{1j}^2}}\left(1 + O\left(\left(\frac{\mu_{1j}}{1-\mu_{1j}^2}\right)^2 I_1 I_j\right)\right)dI_1 dI_j$$

$$\leq N\sum_{j=\bar{j}}^{N}e^{-\frac{1}{2}\frac{(u_{NM}+u_{NM})}{1-\mu_{1j}^2}}\,2(1-\mu_{1j}^2)\big[1 + \mu_{1j}^2\big(u_{NM} + 2(1-\mu_{1j}^2)\big)\big]. \tag{61}$$

B.1 Non-clustering on a Long Range

For a long-range correlation between points, we use that $\mu_{1j} \leq |1-j|^{-\alpha}$. Therefore, recalling that $u_{NM} = 2\log(NM)$ and writing $\mu_0 = \max_{\{j>\bar{j}\}}\mu_{1j}$ the inequality can further simplified by

$$\leq N\sum_{j=\bar{j}}^{N}e^{\frac{-u_{NM}}{1-\mu^2}}\,2(1-\mu^2)\big[1 + |1-j|^{-2\alpha}\big(u_{NM} + 2(1-\mu^2)\big)\big]$$

$$\leq \frac{c}{M^{\frac{2}{1-\mu_0^2}}}\left(\frac{N^2}{N^{\frac{2}{1-\mu_0^2}}} + \frac{N}{N^{\frac{2}{1-\mu_0^2}}}\sum_{j=\bar{j}}^{N}\frac{1}{j^{2\alpha}}\log(NM)^2\right)$$

$$\leq \frac{c}{M^{\frac{2}{1-\mu_0^2}}}\left(\frac{N^2}{N^{\frac{2}{1-\mu_0}}} + \frac{N}{N^{\frac{2}{1-\mu_0}}}\frac{\log(NM)^2}{N^{2\alpha-1}}\right) = o\left(\frac{1}{M}\right) \tag{62}$$

as $N \to \infty$, provided that $\alpha > 0$ (see below the discussion on the decay of correlations).

B.2 Non-clustering in the Vicinity of a Speckle Maximum

Let us now concentrate on the first sum:

$$N\sum_{j=2}^{\bar{j}}\int_{u_{NM}}^{\infty}\int_{u_{NM}}^{\infty}e^{-\frac{1}{2}\frac{(I_1+I_j)}{1-\mu_{1j}^2}}\mathcal{I}_0\left(\frac{\mu_{1j}}{1-\mu_{1j}^2}\sqrt{I_1 I_j}\right)dI_1 dI_j \tag{63}$$

where we take $\bar{j} \leq M$, saying that it is the number of indices for which correlation cannot be neglected.

For values of μ_{1j} close to unity the integral kernel, defined above by $\mathcal{K}(I_1, I_j)$ simplifies considerably due to $1 - \mu_j^2 \ll 1$ such that the sum in expression (63) hence reads

$$\mathcal{K}(I_1, I_j) \leq \frac{\exp\{-\frac{1}{2}\frac{I_1+I_j-2\mu_j\sqrt{I_1 I_j}}{1-\mu^2}\}}{\sqrt{\frac{2\pi\mu_j}{1-\mu_j^2}\sqrt{I_1 I_j}}}\left(1 + O\left(\frac{1-\mu_j^2}{\mu\sqrt{I_1 I_j}}\right)\right). \tag{64}$$

Using the inequality $\sqrt{I}_1\sqrt{I}_j \leq \frac{1}{2}(I_1 + I_j)$ this simplifies expression (63) to

$$\leq N\sum_{j=2}^{\bar{j}} \frac{\sqrt{1-\mu_j^2}(1+\mu_j)^2}{\sqrt{2\pi\mu_j u_{NM}}} e^{-\frac{u_{NM}}{1+\mu_j}} \leq N\sum_{j=2}^{\bar{j}} \frac{\sqrt{1-\mu_j^2}(1+\mu_j)^2}{\sqrt{4\pi\mu_j \log(NM)}} N^{\frac{\mu_j-1}{1+\mu_j}} M^{\frac{-2}{1+\mu_j}} \tag{65}$$

the latter with $u_{NM} = 2\log(NM)$. Now we write $\mu_{1j} = \mu_j = 1 - j^2/k^2$ with $j \leq \bar{j}$, for which the delimiting correlation is denoted by $\bar{\mu} = 1 - \bar{j}^2/k^2$ (for instance of the order of $1/2$). The parabolic dependence of μ on the distance, represented by j/k is typical for any valid speckle correlation function close to $\mu = 1$. The procedure applied here, although being one-dimensional, is applicable to each direction because of the parabolic behaviour in any direction close to $\mu = 1$. Anisotropy [18] is unimportant because each dimension can be normalized by its characteristic (correlation) length. The sum hence reads

$$\leq \frac{1}{\sqrt{4\pi\log(NM)}} \sum_{j=2}^{\bar{j}} \frac{\sqrt{j^2/k^2}}{\sqrt{1-j^2/k^2}} \frac{(2-j^2/k^2)^2}{M(NM)^{\frac{j^2/k^2}{2-j^2/k^2}}}. \tag{66}$$

The latter expression is a Riemann sum and can be replaced sufficiently well by an integral

$$\leq \frac{1}{\sqrt{4\pi\log(NM)}} \frac{1}{M} k \int_{\xi=0}^{\sqrt{\bar{\mu}}} d\xi^2 \frac{(2-\xi^2)^2}{\sqrt{1-\xi^2}} (NM)^{-\frac{\xi^2}{2-\xi^2}}. \tag{67}$$

The integral itself yields a weak dependence $(NM)^{\gamma(\bar{\mu})}$ of NM with an exponent depending on $\bar{\mu} \lesssim 0.2$ typically $\gamma(\bar{\mu} = 0.5) \simeq 0.1$, such that the inequality yields eventually

$$\leq \frac{k}{2M\sqrt{\pi\log NM}} (NM)^{\gamma(\bar{\mu})} \leq \frac{1}{M^{1+\epsilon}}. \tag{68}$$

The criterion for non-clustering cannot be fulfilled if the left-hand-side does not converge such that $0 < \epsilon < 1$ can be found. This final expression has to be evaluated, first, for the upper limit of the k value, being the number of grid points in one direction over a typical correlation length r_c of the speckle correlation function, thus $k_{\max} = r_c/\Delta x$ which is as well $k_{\max} = r_c n_x/L_x$ for a mesh of n_x grid points over the box length L_x. For a symmetric mesh, for instance, the total number of grid points is $n_{\text{grid}} = n_x^d$ in dimension d ($d = 2$ for 2D and $d = 3$ for 3D geometry). The generalisation to $d = 2$ and $d = 3$ is justified, as already mentioned above, by the fact that we can assume isotropy in the vicinity of the speckle peak because of the parabolic behaviour around this point (with characteristic lengths in each direction). Normalizing the directions with respect to their characteristic length, we can express the specific volume of a speckle to a typical length r_c^d, such that the number of speckles in the box hence $n_{\text{sp}} \simeq (L/r_c)^d$, results in $k_{\max} = (n_{\text{grid}}/n_{\text{sp}})^{1/d}$.

In a similar way we can define k in general for a number of points $NM < n_{\mathrm{grid}}$, namely $k = (NM/n_{\mathrm{sp}})^{1/d}$. This helps to evaluate the above expression for a valid criterion (68) on the non-clustering property. With the above dependence of k on the number of points NM reads

$$\frac{(NM)^{1/d-\gamma(\bar{\mu})}}{2\sqrt{\pi \log NM}} \leq \frac{n_{\mathrm{sp}}^{1/d}}{M^{\epsilon}}.$$

The criterion is easily fulfilled for $n_{\mathrm{sp}} > NM$.

Leadbetter [28] has developed a criterion that allows to determine the parameter θ of the Gumbel law. The validity of isotropy in the vicinity of the speckles allows furthermore the consideration of a single θ value (see [18]). The first approximation, that consists in neglecting the exceedences higher than of the order of two, yields the expression

$$\frac{k}{2\sqrt{\pi \log NM}}(NM)^{\gamma(\bar{\mu})} - (1-\theta) = 0. \tag{69}$$

If the non-clustering condition is fulfilled, this leads to a θ value of $\theta = 1$, otherwise θ can roughly be estimated to decrease towards small positive values like

$$\theta \simeq 1 - k\frac{(NM)^{-\gamma(\bar{\mu})}}{2\sqrt{\pi \log NM}} \simeq 1 - \frac{(NM)^{1/d-\gamma(\bar{\mu})}}{2(n_{\mathrm{sp}})^{1/d}\sqrt{\pi \log NM}}. \tag{70}$$

The value of θ shifts, see (14) and (16), by $\log\theta$, the center of the Gumbel distribution in the intensity. Leadbetter shows [28] that a more precise analysis of θ developed as a function of the order of exceedences can be performed. We have determined θ from numerical simulations as a function of NM that (1) shows a good agreement with the above expression for $4n_{\mathrm{sp}} > NM > n_{\mathrm{sp}}$. For the concrete case discussed in Sect. 2.3, the value of $NM \equiv n$ denotes the total number of points considered for the sequence $I_1, \ldots, I_n$, and N the number of speckles n_{sp}. Hence, it follows $\theta NM/n_{\mathrm{sp}} = \theta M = const$ for $NM \gg n_{\mathrm{sp}}$ and with $\theta = 1$ for $NM < n_{\mathrm{sp}}$, being the non-clustering case.

Appendix C: Proof for the Mixing Condition

In the following we present a sketch of the proof for the mixing condition. We have

$$\begin{aligned} &|P(I_{i_1} < u_{i_1}, \ldots, I_{i_k} < u_{i_k}, I_{j_1} < u_{j_1}, \ldots, I_{j_t} < u_{j_t}) \\ &\quad - P(I_{i_1} < u_{i_1}, \ldots, I_{i_k} < u_{i_k}) P(I_{j_1} < u_{j_1}, \ldots, I_{j_t} < u_{j_t})|. \end{aligned} \tag{71}$$

Similar to the result from Appendix A, but for different integral bounds, we proceed

$$\begin{aligned} \leq \Bigg| &\int_0^{u_{i_1}} \ldots \int_0^{u_{j_t}} e^{-\frac{1}{2}\sum_{i=1}^{k+t}\lambda_i I_i} \Bigg(\prod_{(i,j),\binom{k+t}{2}\text{ terms}} \mathcal{I}_0(\mu_{ij}\sqrt{I_i I_j}) + \sum\prod \mathcal{I}_{k_l} \Bigg) dI_1 \ldots dI_k \ldots dI_t \\ &- \int_0^{u_{i_1}} \ldots \int_0^{u_{i_k}} e^{-\frac{1}{2}\sum_{i=1}^{k}\lambda_i I_i} \Bigg(\prod_{(i,j),\binom{k}{2}\text{ terms}} \mathcal{I}_0(\mu_{ij}\sqrt{I_i I_j}) + \sum\prod \mathcal{I}_{k_l} \Bigg) dI_1 \ldots dI_k \\ &\cdot \int_0^{u_{j_1}} \ldots \int_0^{u_{j_k}} e^{-\frac{1}{2}\sum_{i=1}^{t}\lambda_i I_i} \Bigg(\prod_{(i,j),\binom{t}{2}\text{ terms}} \mathcal{I}_0(\mu_{ij}\sqrt{I_i I_j}) + \sum\prod \mathcal{I}_{k_l} \Bigg) dI_1 \ldots dI_t \Bigg| \end{aligned} \tag{72}$$

recalling that since $i_k + n < j_1$, the μ_{ij} decrease as $|i-j|^{-\alpha} \le 1/s^a$, $a = 1$.

Again with $\binom{k+t}{2} = \binom{k}{2} + \binom{t}{2} + \binom{k}{1}\binom{t}{1}$ the correlations split into first block, second block, and between blocks (separated by s) correlations, so that the difference can be estimated as

$$\begin{aligned}
&\le \int_0^\infty \dots \int_0^\infty dI_1 \dots dI_k \dots dI_t e^{-\frac{1}{2}\sum_{i=1}^k \lambda_i I_i} e^{-\frac{1}{2}\sum_{i=1}^t \lambda_i I_i} \\
&\cdot \left(\prod_{(i,j),(k)(k-1)/2\,\text{terms}} \mathcal{I}_0(\mu_{ij}\sqrt{I_i I_j}) + \sum \prod \mathcal{I}_{k_l}(\dots) \right) \\
&\cdot \left(\prod_{(i,j),(t)(t-1)/2\,\text{terms}} \mathcal{I}_0(\mu_{ij}\sqrt{I_i I_j}) + \sum \prod \mathcal{I}_{k_l}(\dots) \right) \\
&\cdot \left| \prod_{(i,j),kt\ \text{terms}} \mathcal{I}_0(\mu_{ij}\sqrt{I_i I_j}) + \sum \prod \mathcal{I}_{k_l}(\dots) - 1 \right| \qquad (73)
\end{aligned}$$

since the difference $\prod_{(i,j),kt\ \text{terms}} \mathcal{I}_0(\mu_{ij}\sqrt{I_i I_j}) + \sum \prod \mathcal{I}_{k_l}(\dots) - 1$ is positive. The slowest term in the difference in (73) is given by the product of $\mathcal{I}_0$'s; so we are led to compute integrals of the form:

for $n = 2$ it is $k = 1$ and $t = 1$:

$$\int_0^\infty \int_0^\infty e^{-(aI_1+bI_2)} \big(\mathcal{I}_0(\alpha\sqrt{I_1 I_2}) - 1\big) dI_1 dI_2$$

for $n = 3$, take e.g. $k = 2$ and $t = 1$:

$$\int_0^\infty \int_0^\infty \int_0^\infty e^{-(aI_1+bI_2+cI_3)} \mathcal{I}_0(\alpha\sqrt{I_1 I_2}) \big(\mathcal{I}_0(\beta\sqrt{I_1 I_3})\mathcal{I}_0(\gamma\sqrt{I_2 I_3}) - 1\big) dI_1 dI_2 dI_3.$$

Using that $\int_0^\infty x \exp(-ax^2)\mathcal{I}_0(\alpha x)\mathcal{I}_0(\beta x)dx = (1/2a)\exp\{(\alpha^2+\beta^2)/4a\}\mathcal{I}_0(-\alpha\beta/2a)$ and that $\int_0^\infty x \exp\{-ax\}\mathcal{I}_0(\alpha x)dx = (a^2-\alpha^2)^{-1/2}$ yields for $n = 2$

$$\int_0^\infty \int_0^\infty e^{-(aI_1+bI_2)} \big(\mathcal{I}_0(\alpha\sqrt{I_1 I_2}) - 1\big) dI_1 dI_2 = \frac{1}{b}\frac{1}{a - (\alpha^2/2b)} - \frac{1}{ab}$$

so that the difference goes to zero as α^2 that is, as the square of the correlation μ.

For $n = 3$ we have chosen $k = 2$ and $t = 1$ so that I_1 and I_2 are in the same group, and I_3 in the other that is I_1 and I_2 are "near" each of the other, and both "far" from I_3, so that here we wish to estimate the decay to zero as γ and β go to zero. This yields

$$\begin{aligned}
&\int_0^\infty dI_2 \int_0^\infty dI_3\, e^{-(bI_2+cI_3)} \mathcal{I}_0(\gamma\sqrt{I_2 I_3}) \int_0^\infty e^{-(aI_1)} \mathcal{I}_0(\alpha\sqrt{I_1 I_2})\mathcal{I}_0(\beta\sqrt{I_1 I_3}) dI_1 \\
&= \frac{1}{ab - \alpha^2/4} \left(\sqrt{c - \beta^2/4a - \left(a\frac{\gamma^2 + (\alpha^2\beta^2/4a^2)}{4ab - \alpha^2} \right)^2 - 4a^2 \frac{\alpha^2\beta^2\gamma^2}{(4ab-\alpha^2)^2}} \right)^{-1/2}
\end{aligned}$$

and

$$\int_0^\infty dI_2 dI_3 \int_0^\infty e^{-(bI_2+cI_3)} \int_0^\infty e^{-(aI_1)} \mathcal{I}_0(\alpha\sqrt{I_1 I_2}) dI_1 = \frac{1}{ac}\frac{1}{b - \alpha^2/4a}.$$

The difference for $n = 3$ goes to zero as $-1 + [1 + \gamma^2 + \beta^2]^{-1/2}$, that is as the square of correlations μ, hence, the mixing property is satisfied with $\alpha(n) \to 0$ as $n \to \infty$: the coefficients $\alpha(n)$ decrease to 0 as μ_{1n}^2, that is as $(\frac{1}{n})^a$ $(a = 2)$, see Sect. 5.

For n larger, we have to compute integrals of the form

$$\int_0^\infty te^{-at^2}\mathcal{I}_0(\alpha t)\mathcal{I}_0(\beta t)\mathcal{I}_0(\gamma t)dt$$

where three (or more) Bessel function of the same order are involved.

Making use of the formula [35]

$$\mathcal{J}_0(\alpha t)\mathcal{J}_0(\beta t) = (1/\pi)\int_0^\pi \mathcal{J}_0(t\sqrt{\alpha^2+\beta^2-2\alpha\beta\cos\phi})d\phi$$

we can evaluate the integrals:

$$\int_0^\infty te^{-at^2}\mathcal{I}_0(\alpha t)\mathcal{I}_0(\beta t)\mathcal{I}_0(\gamma t)dt$$
$$= \frac{e^{\frac{\alpha^2+\beta^2+\gamma^2}{4a^2}}}{2\pi a^2}\int_0^\pi e^{\frac{\alpha\beta\gamma\cos\phi}{4a^2}}\mathcal{I}_0\left(\frac{\alpha\sqrt{\beta^2+\gamma^2-2\beta\gamma\cos\phi}}{2a^2}\right)d\phi \tag{74}$$

by making use, via induction, of the known formula [35] for the integral containing the product of two Bessel functions $\int_0^\infty te^{-at^2}\mathcal{I}_0(\alpha t)\mathcal{I}_0(\beta t)dt = (1/2a^2)\exp\{(\alpha^2+\beta^2)/4a^2\} \times \mathcal{I}_0(\alpha\beta/2a^2)$.

Using now the Graf formula $\mathcal{I}_0(\sqrt{\beta^2+\gamma^2-2\beta\gamma\cos\phi}) = \sum_0^\infty \epsilon_k\mathcal{I}_k(\beta)\mathcal{I}_k(\gamma)\cos k\phi$ and $\int_0^\pi e^{a\cos\phi}\cos k\phi d\phi = \pi\mathcal{I}_k(a)$ we find the nice formula:

$$\int_0^\infty te^{-at^2}\mathcal{I}_0(\alpha t)\mathcal{I}_0(\beta t)\mathcal{I}_0(\gamma t)dt = \frac{1}{2a^2}e^{\frac{\alpha^2+\beta^2+\gamma^2}{4a^2}}\sum_{k=0}^\infty \mathcal{I}_k\left(\frac{\alpha\gamma}{2a^2}\right)\mathcal{I}_k\left(\frac{\alpha\beta}{2a^2}\right)\mathcal{I}_k\left(\frac{\beta\gamma}{2a^2}\right). \tag{75}$$

This is an inductive procedure that allows theoretically to perform integrals of the type containing products of Bessel functions; in practice, formulas at higher order become too complicated. Nevertheless is clear from this result that the successive formulae contain products of Bessel functions of higher order, whose decay to zero is faster with larger order, so that the speed of convergence is given by the first terms containing the 0-th order Bessel function, the argument of which argument contains the correlation coefficient μ_{ij} between two points, hence the decay goes as the square of μ_{ij}.

References

1. Rose, H.A., DuBois, D.F.: Laser hot spots and the breakdown of linear instability theory with application to stimulated Brillouin scattering. Phys. Rev. Lett. **72**, 2883 (1994)
2. Hüller, S., Mounaix, Ph., Tikhonchuk, V.T.: SBS reflectivity from spatially smoothed laser beam: Random phase plates versus polarization smoothing. Phys. Plasmas **5**, 2706 (1997)
3. Mounaix, Ph., Divol, L., Hüller, S., Tikhonchuk, V.T.: Effects of spatial and temporal smoothing on stimulated Brillouin scattering in the independent-hot-spot model limit. Phys. Rev. Lett. **85**, 4526 (2000)
4. Pesme, D., Hüller, S., Myatt, J., Riconda, C., Maximov, A., Tikhonchuk, V.T., Labaune, C., Fuchs, J., Depierreux, S., Baldis, H.A.: Laser-plasma interaction studies in the context of megajoule lasers for inertial fusion. Plasma Phys. Control. Fusion **44**, B53 (2002)

5. Ohtsubo, J., Asakura, A.: Statistical properties of laser speckle produced in the diffraction field. Appl. Opt. **16**, 1742 (1977)
6. Ohtsubo, J., Asakura, A.: Statistical properties of the sum of partially developed speckle patterns. Opt. Lett. **1**, 98 (1977)
7. Kato, Y., Mima, K., Miyanaga, N., Arinaga, S., Kitagawa, Y., Nakatsuka, M., Yamanaka, C.: Random phasing of high-power lasers for uniform target acceleration and plasma-instability suppression. Phys. Rev. Lett. **53**, 1057 (1984)
8. Obenschain, S.P., Grun, J., Herbst, M.J., Kearney, K.J., Manka, C.K., McLean, E.A., Mostovych, A.N., Stamper, J.A., Whitlock, R.R., Bodner, S.E., Gardner, J.H., Lehmberg, R.H.: Laser-target interaction with induced spatial incoherence. Phys. Rev. Lett. **56**, 2807–2810 (1986)
9. Goodman, J.: Statistical Optics. Wiley, New York (1985)
10. Goodman, J.: Statistical properties of laser speckle patterns. In: Topics in Applied Physics. Laser Speckle and Related Phenomena, vol. 9, pp. 9–74. Springer, Berlin (1984)
11. Rose, H.A., Dubois, D.F.: Statistical properties of hot spots produced by a random phase plate. Phys. Fluids B **5**, 590 (1993)
12. Biancalana, V., Chessa, P.: Handling of quasi-Gaussian beams by phase plates: far-field simulation. Appl. Opt. **33**, 3465–3477 (1994)
13. Tikhonchuk, V.T., Labaune, C., Baldis, H.A.: Modeling of a stimulated Brillouin scattering experiment with statistical distribution of speckles. Phys. Plasmas **3**, 3777 (1996)
14. Tikhonchuk, V.T., Fuchs, J., Labaune, C., Depierreux, S., Hüller, S., Myatt, J., Baldis, H.A.: Stimulated Brillouin and Raman scattering from a randomized laser beam in large inhomogeneous plasmas. II: Model description and comparison with experiments. Phys. Plasmas **8**, 1636 (2001)
15. Masson-Laborde, P.E., Hüller, S., Pesme, D., Casanova, M., Loiseau, P.: Modeling parametric scattering instabilities in large-scale expanding plasmas. J. Phys. IV France **133**, 247 (2006)
16. Middleton, D.: An Introduction to Statistical Communications Theory. Wiley, New York (1960)
17. Adler, R.J.: The Geometry of Random Fields. Wiley, New York (1981)
18. Adler, R.J.: An Introduction to Continuity, Extrema, and Related Topics for General Gaussian Processes. Lecture Notes Monograph Series. Institute of Mathematical Statistics, Beachwood (1990)
19. Garnier, J.: Statistical properties of the hot spots of smoothed beams produced by random phase plates revisited. Phys. Plasmas **6**, 1601 (1999)
20. Garnier, J., Gouedard, C., Migus, A.: Statistics of the hottest spot of speckle patterns generated by smoothing techniques. J. Mod. Opt. **46**, 1213 (1999)
21. Embrechts, P., Kluppelberg, C., Mikosch, T.: Modelling Extremal Events. Springer, Berlin (1997)
22. Fisher, R.A., Tippett, L.H.C.: Limiting forms of the frequency distribution of the largest or smallest number of a sample. Proc. Camb. Philos. Soc. **24**, 180–190 (1928)
23. Berman, S.: Limit theorems for the maximum term in stationary sequences. Ann. Math. Stat. **35**, 502–516 (1964)
24. Galambos, J.: The Asymptotic Theory of Extreme Order Statistics. Wiley, New York (1978)
25. Gnedenko, B.V.: Sur la distribution limite du terme maximum d'une serie aleatoire. Ann. Math. **44**, 423–453 (1943)
26. Gumbel, E.J.: Statistics of Extremes. Columbia Univ. Press, New York (1959)
27. Leadbetter, M.R., Lindgren, G., Rootzen, H.: Extreme and Related Properties of Random Sequences and Processes. Springer, Berlin (1982)
28. Leadbetter, M.R.: Extreme and Local Dependence in stationary sequences. Z. Wahrscheinlichkeitstheor. Verw Geb. **65**, 291–306 (1983)
29. Jaffard, S.: Proprietés des matrices bien localisées près de leur diagonale et quelques applications. Ann. IHP C **7**(5), 461–476 (1990)
30. Grenander, U., Szegö, G.: Toeplitz Forms and Their Applications. Chelsea, New York (1984)
31. Gray, R.M.: Toeplitz and Circulant Matrices: A Review. Foundations and Trends in Communications and Information Theory, vol. 2(3), pp. 155–239. Now Publishers, Hannover (2006)
32. Rio, E.: Théorie Asymptotique des Processus Aléatoires Faiblements Dépendants. Springer, New York (2000)
33. Hsing, T.: A note on the asymptotic independence of the sum and the maximum of strongly mixing stationary random variables. Ann. Probab. **23**, 938–947 (1995)
34. Mounaix, Ph., Divol, L.: Near-threshold reflectivity fluctuations in the independent-convective-hot-spot-model limit of a spatially smoothed laser beam. Phys. Rev. Lett. **89**, 165005 (2002)
35. Watson, G.N.: A Treatise on the Theory of Bessel Functions. Cambridge University Press, Cambridge (1995)